Overview of the latest ATLAS and ATLAS-AFP photoproduction results

André Sopczak

IEAP CTU in Prague

on behalf of the ATLAS Collaboration

LHC Diffraction and Low-x 2024

11 September 2024

Reference	Date	√s (TeV)	L	Links
https://twiki.cern.ch/twiki/bin/view/AtlasPublic				
Search for magnetic monopoles in Pb+Pb UPC	HION	Submitted to PRL	2024-08-20	5.36/NN	262 µb-1	Documents | 2408.11035 Inspire | Internal
Electroweak, QCD and flavour physics studies	STDM	Submitted to Physics Reports	2024-04-10	13	140 fb^{-1}	Documents | 2404.06829 Inspire | Internal
Charged hadron yields in photonuclear collisions	HION	ATLAS-CONF-2023-059	2023-09-04	5.02/NN	1.7 nb-1	Documents | Internal
Diphoton resonance search with AFP tag	EXOT	JHEP 07 (2023) 234	2023-04-21	13	30 fb^{-1}	Documents | 2304.10953 Inspire | HepData | Internal
Observation of the $\gamma\gamma \rightarrow \tau\tau$ process and constraints on the tau-lepton anomalous magnetic moment	STDM	Phys. Rev. Lett. 131 (2023) 151802	2022-04-28	5.02/NN	1.73 nb^{-1}	Documents | 2204.13478 Inspire | Briefing | Internal
Measurements of jet production in ultra-peripheral collisions	HION	ATLAS-CONF-2022-021	2022-04-02	5.02/NN	2 nb-1	Documents | Internal
Observation of photon-induced WW production	STDM	Phys. Lett. B 816 (2021) 136190	2020-10-08	13	139 fb^{-1}	Documents | 2010.04019 Inspire | Briefing | Internal
Differential light-by-light and ALP search in PbPb at 5.02 TeV	HION	JHEP 03 (2021) 243	2020-08-12	5.02/NN	1.75 nb^{-1}, 0.49 nb^{-1}	Documents | 2008.05355 Inspire | HepData Internal
Observation of forward proton scattering in association with lepton pairs produced in photon fusion	STDM	Phys. Rev. Lett. 125 (2020) 261801	2020-09-30	13	14.6 fb^{-1}	Documents | 2009.14537 Inspire | HepData | Briefing Internal
Observation of light-by-light scattering and new results from ultra-peripheral heavy-ion collisions in the ATLAS experiment	HION	Phys. Rev. Lett. 123 (2019) 052001	2019-04-06	5.02/NN	0.5 nb-1, 1 nb-1	Documents | 1904.03536 Inspire | HepData Briefing | Internal
Evidence for light-by-light scattering in 5.02 TeV Pb+Pb	HION	Nature Phys. 13 (2017) 852	2017-02-06	5.02/NN	0.48 nb^{-1}	Documents | 1702.01625 Inspire | HepData | Briefing Internal
Exclusive WW cross-section at 8 TeV	STDM	Phys. Rev. D 94 (2016) 032011	2016-07-13	8	20.3 fb^{-1}	Documents | 1607.03745 Inspire | HepData | Internal
High-mass Drell-Yan differential cross sections at 8 TeV	STDM	JHEP 08 (2016) 009	2016-06-06	8	20.2 fb^{-1}	Documents | 1606.01736 Inspire | HepData | Internal
Exclusive dilepton production at 7 TeV	STDM	Physics Letters B 749 (2015) 242-261	2015-06-23	7	4.6 fb^{-1}	Documents | 1506.07098 Inspire | HepData | Internal

Ultra-peripheral collisions (UPC)

- Program of physics of ultra-peripheral collisions (UPC) has advanced significantly for 10 years of LHC
- Boosted nuclei and strong EM fields: source of quasi-real photons
- $E\max \leq \gamma/R \sim 80$ GeV at LHC $Z^2 (\approx 6.7 \times 10^3)$ enhancement of cross sections for Pb wrt proton beams.
- Precision tool to study photon fluxes
- Instrumentation in the forward region (ZDCs) offers control over backgrounds and impact-parameter dependence
- Large integrated luminosities give access to rare processes, thus a tool to search for physics Beyond Standard Model (BSM)

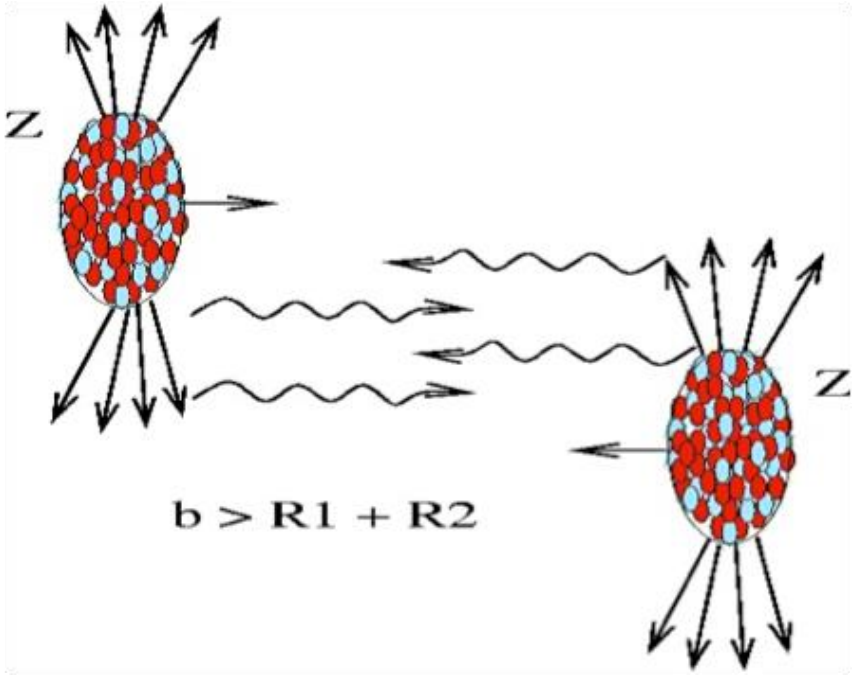

Rare Process

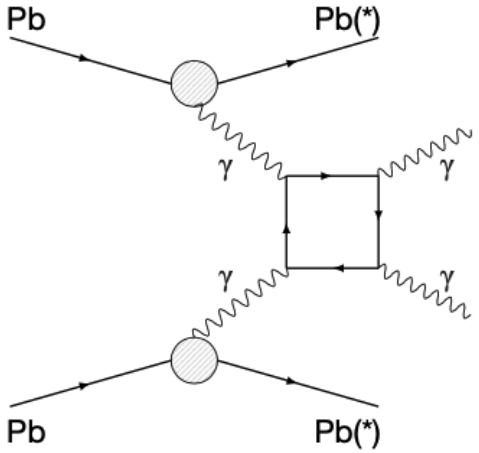

Precision physics

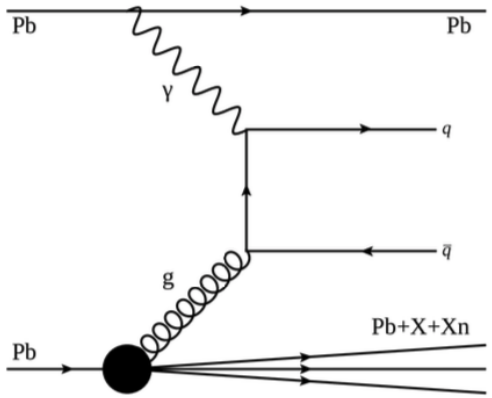

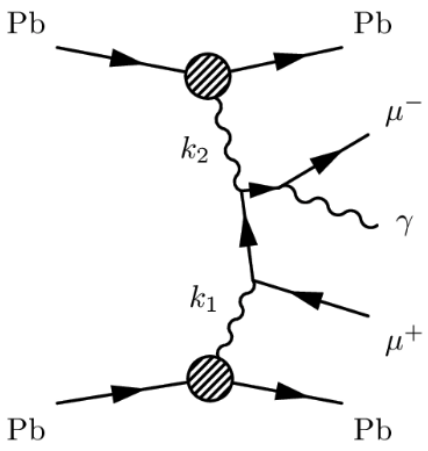

Searches

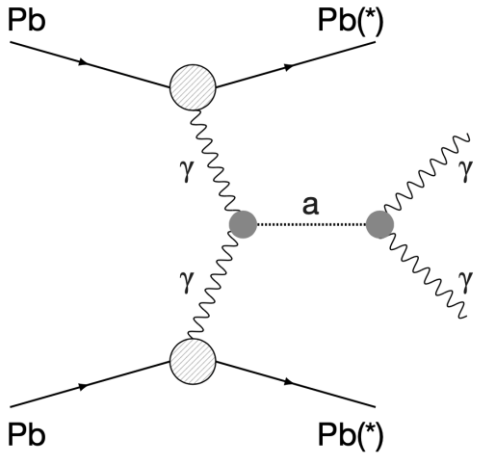

Light-by-light scattering at LHC

Evidence: SM $\gamma\gamma \to \gamma\gamma$ observed in lead ion collisions,
Nature Phys. 13 (2017) 852

SM $\gamma\gamma \to \gamma\gamma$ observed in lead ion collisions

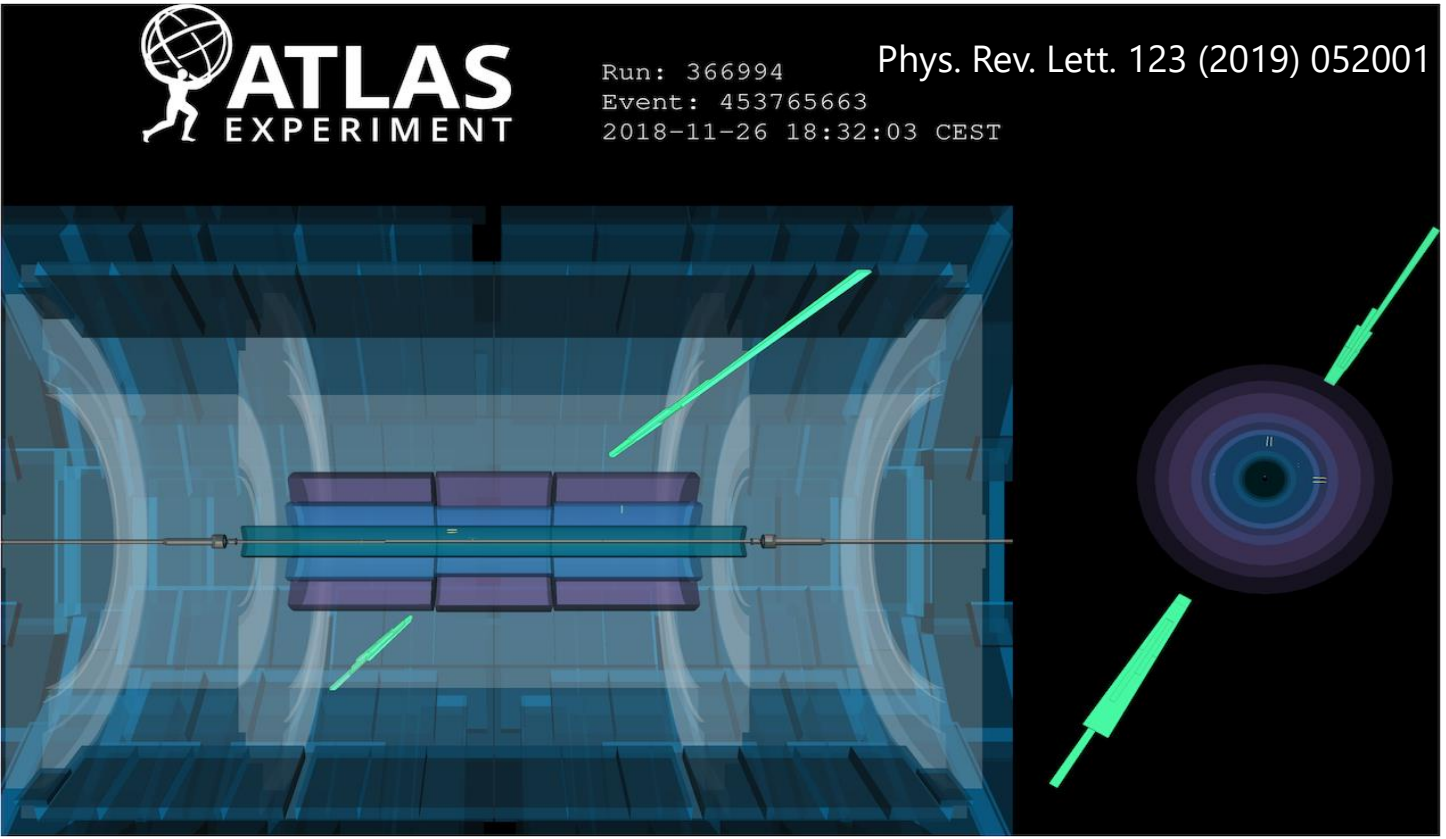

In pp collisions, SM $\gamma\gamma \to \gamma\gamma$ has small cross section…

but BSM can enhance it!

e.g. Axion-like particle (ALP)

Differential light-by-light and Axion-Like Particle in PbPb

JHEP 03 (2021) 243

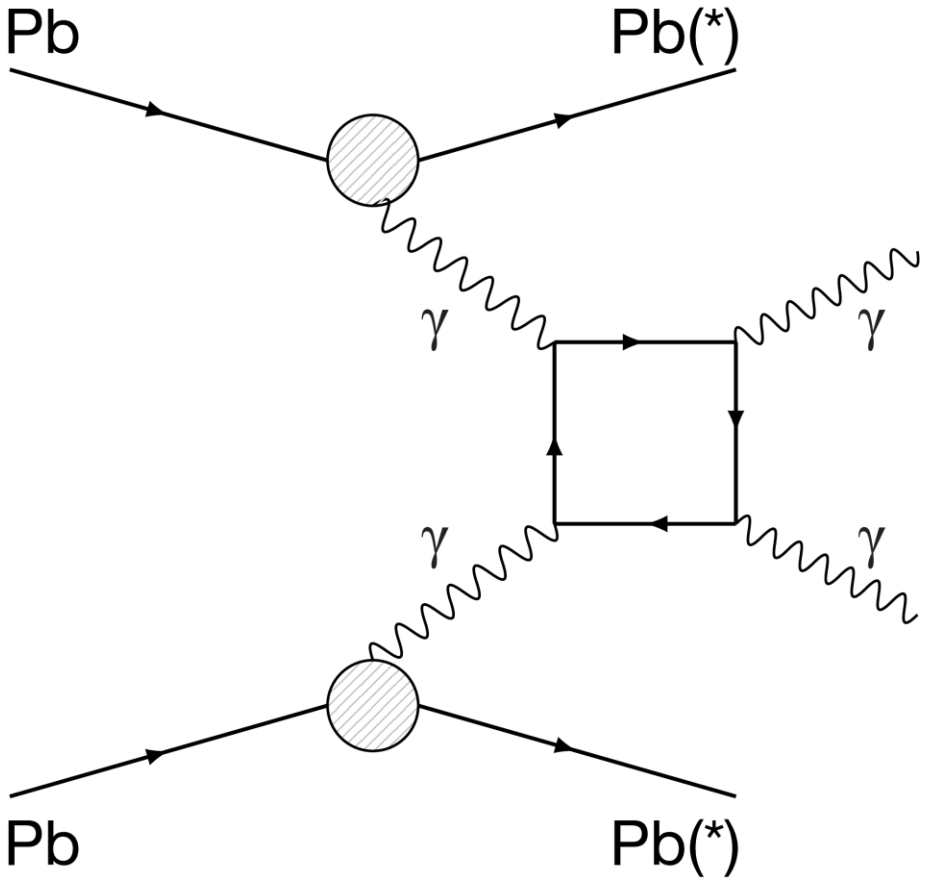

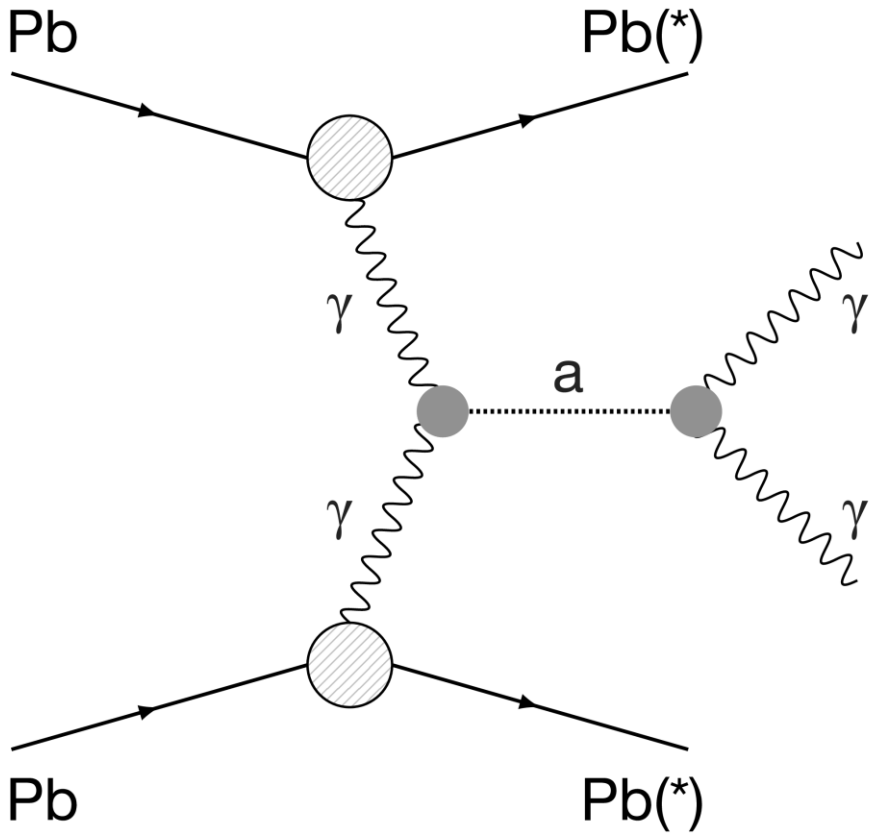

- 2.2 nb^{-1} of Pb+Pb data
- 2015 and 2018 at $\sqrt{s_{NN}}$ = 5.02 TeV

Differential light-by-light and Axion-Like Particle in PbPb

JHEP 03 (2021) 243

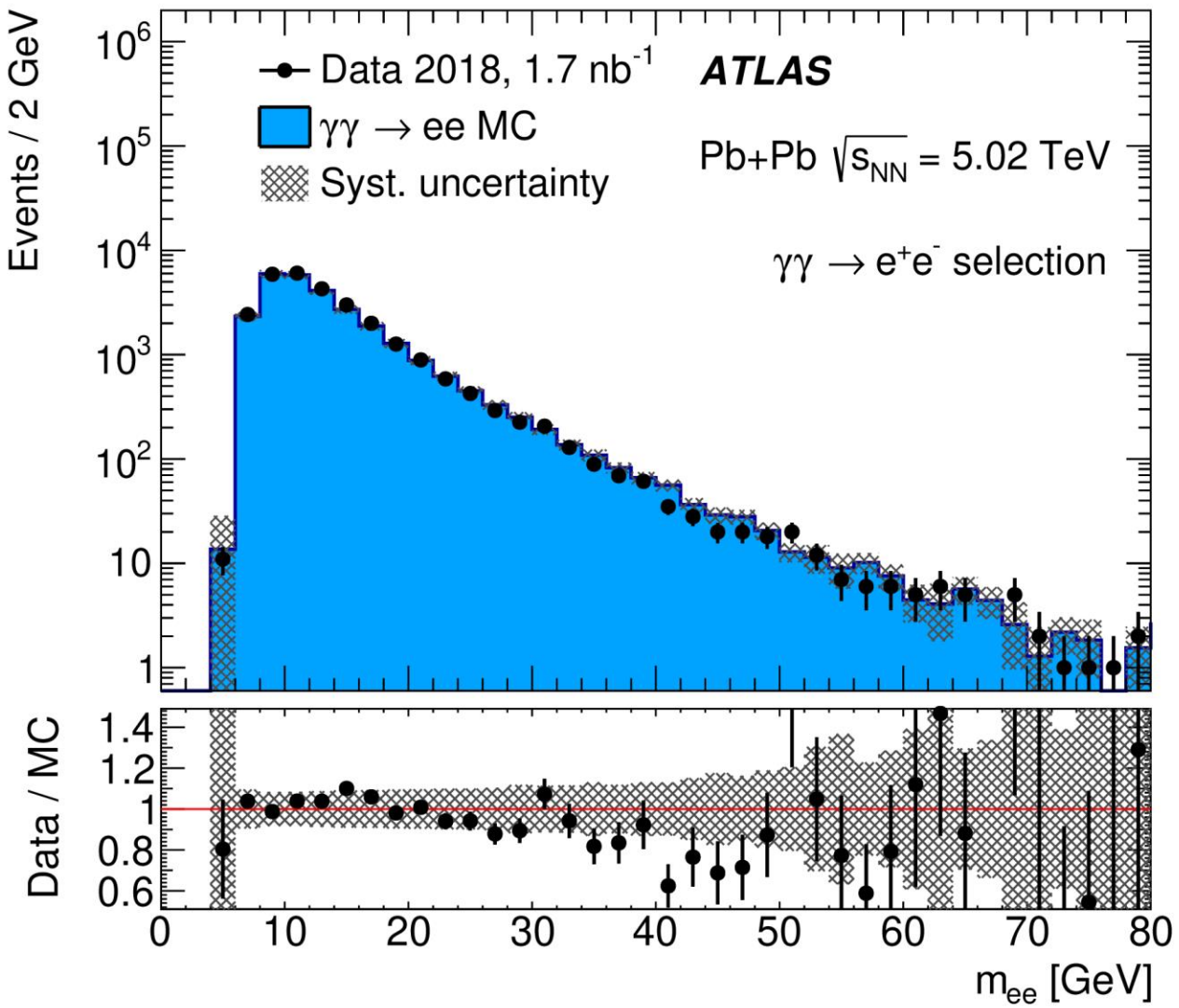

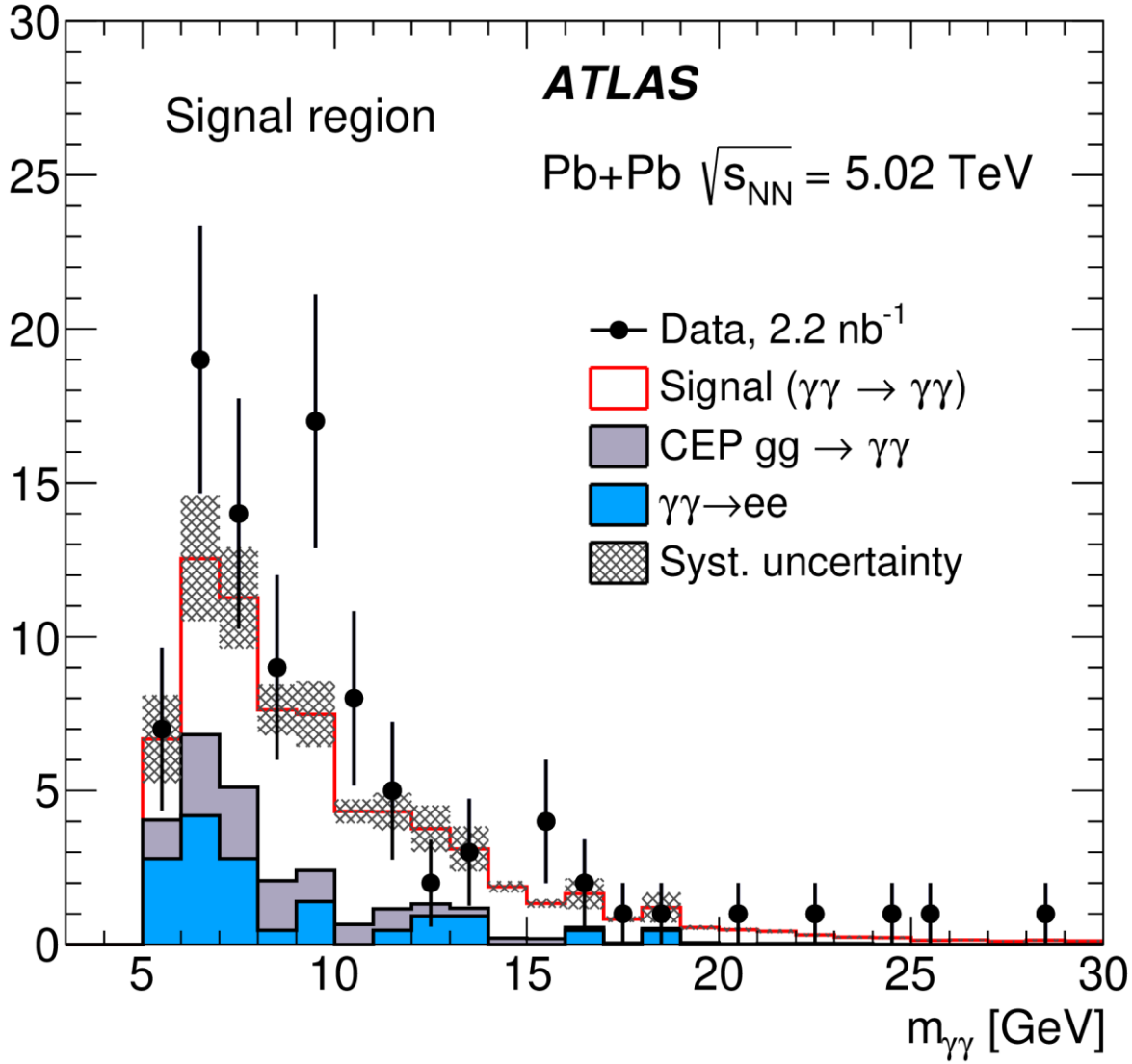

Differential light-by-light and Axion-Like Particle in PbPb

JHEP 03 (2021) 243

Differential fiducial cross sections of $\gamma\gamma \rightarrow \gamma\gamma$ production

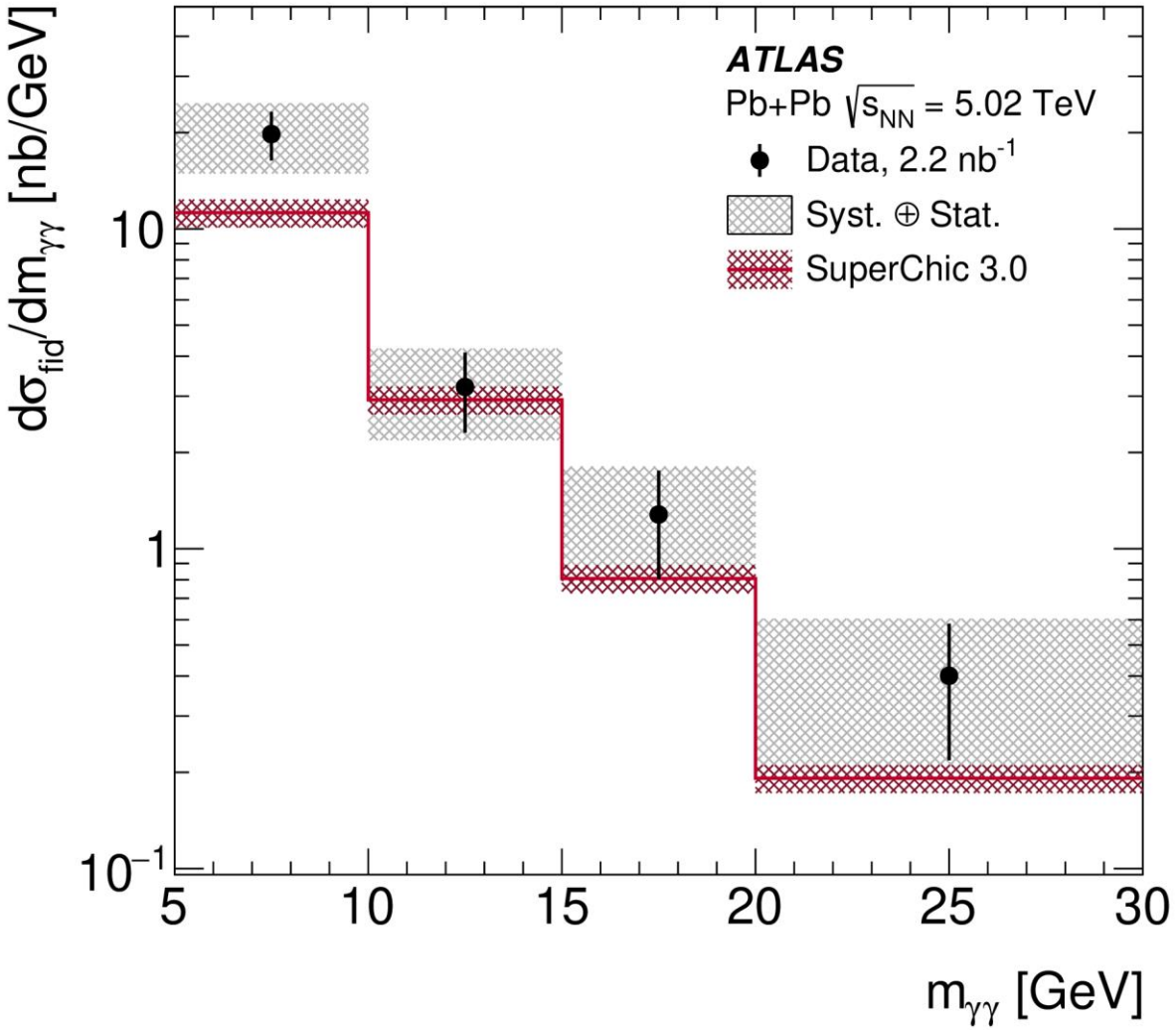

95% CL upper limit on the ALP cross section $\sigma(\gamma\gamma \rightarrow a \rightarrow \gamma\gamma)$ in the mass range 6 to 100 GeV

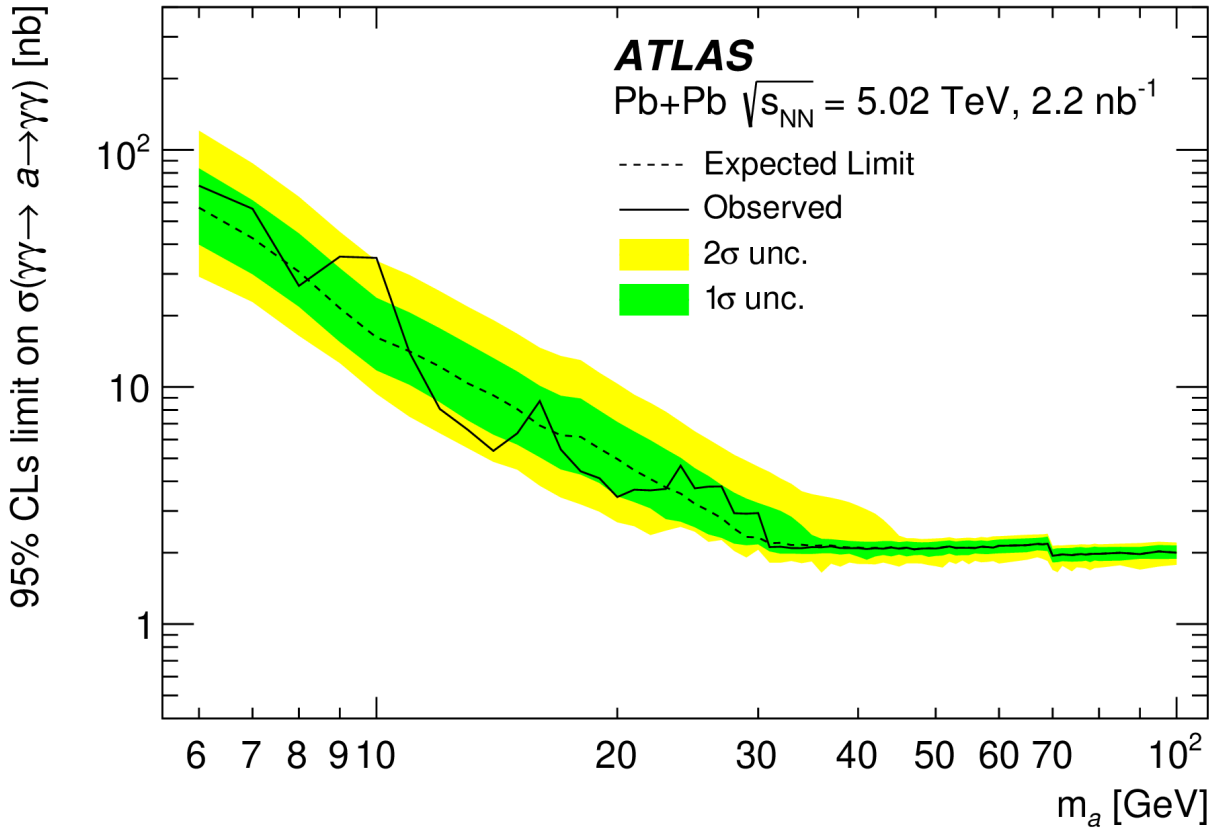

Measurements of jet production in ultra-peripheral collisions

ATLAS-CONF-2022-021

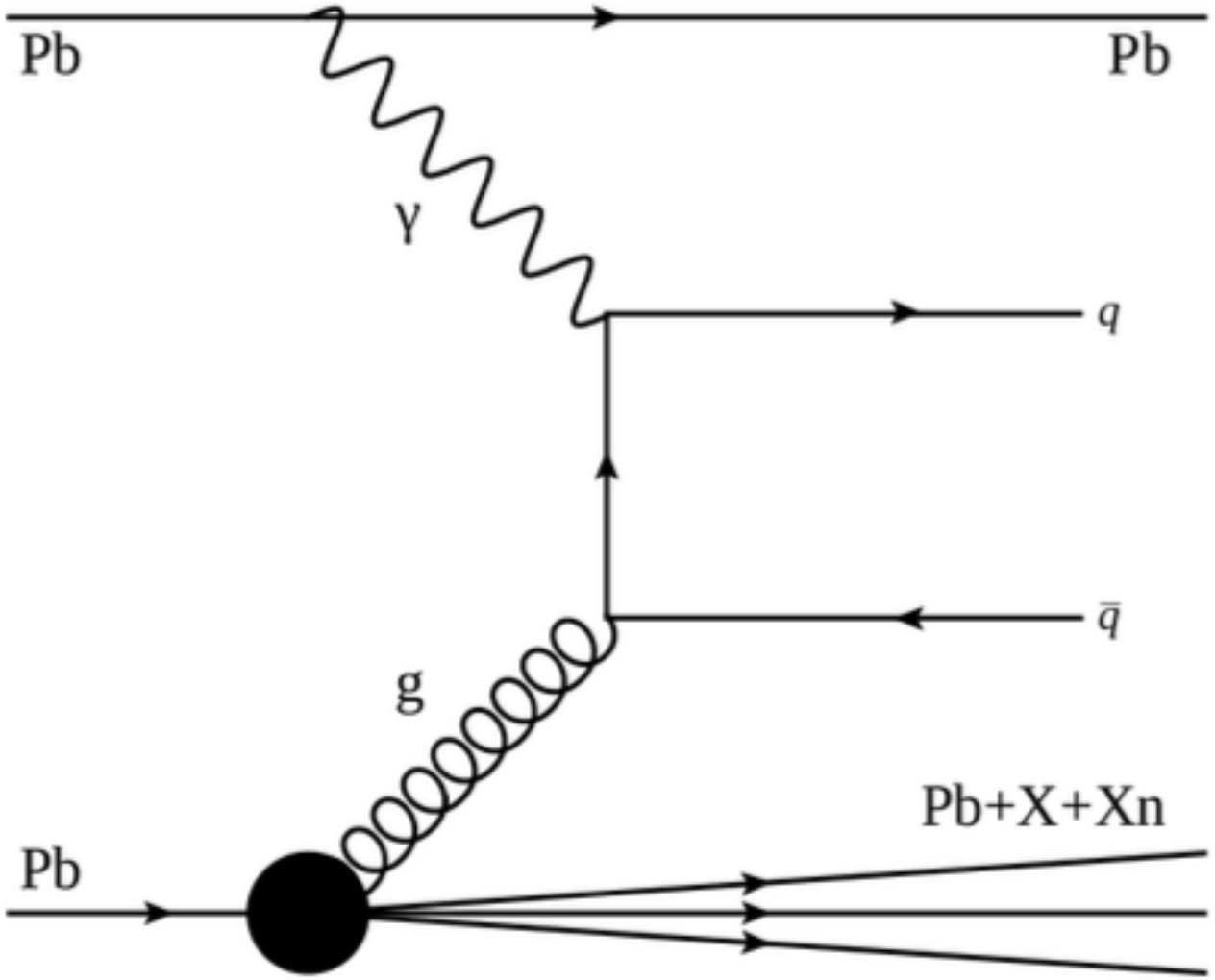

Data set recorded in 2018 with an integrated luminosity of 1.72 nb^{-1}

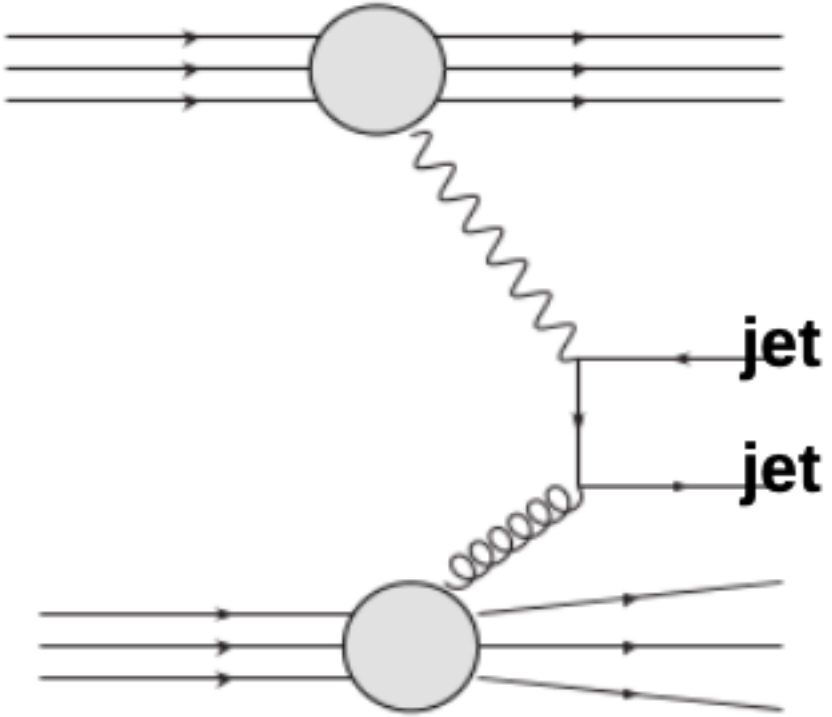

Particle-flow jets are reconstructed using the anti-k_t algorithm with radius parameter, R=0.4.

Measurements of jet production in ultra-peripheral collisions

ATLAS-CONF-2022-021

Observables

$$H_{\mathrm{T}} \equiv \sum_i p_{\mathrm{T}\,i} \longrightarrow \sim Q$$

$$x_{\mathrm{A}} \equiv \frac{m_{\mathrm{jets}}}{\sqrt{s}} e^{-y_{\mathrm{jets}}} \longrightarrow$$ fraction of beam momentum carried by partons **in nucleus** (in "direct" $x_A \sim x$)

$$z_{\gamma} \equiv \frac{m_{\mathrm{jets}}}{\sqrt{s}} e^{+y_{\mathrm{jets}}} \longrightarrow$$ fraction of beam momentum carried by partons **in photon** (in "direct" $z_\gamma \sim$ DIS y)

… where

$$y_{\mathrm{jets}} \equiv \frac{1}{2} \ln \left(\frac{\sum_i E_i + \sum_i p_{z\,i}}{\sum_i E_i - \sum_i p_{z\,i}} \right)$$

$$m_{\mathrm{jets}} \equiv \left[\left(\sum_i E_i \right)^2 - \left| \sum_i \vec{p}_i \right|^2 \right]^{1/2}$$

… *i* goes through all the jets

Measurements of jet production in ultra-peripheral collisions

ATLAS-CONF-2022-021

Triple-differential cross-sections measured as a function of the nuclear and photon parton momentum fractions, x_A and z_γ, respectively, and the total transverse momentum in the jet system, H_T.

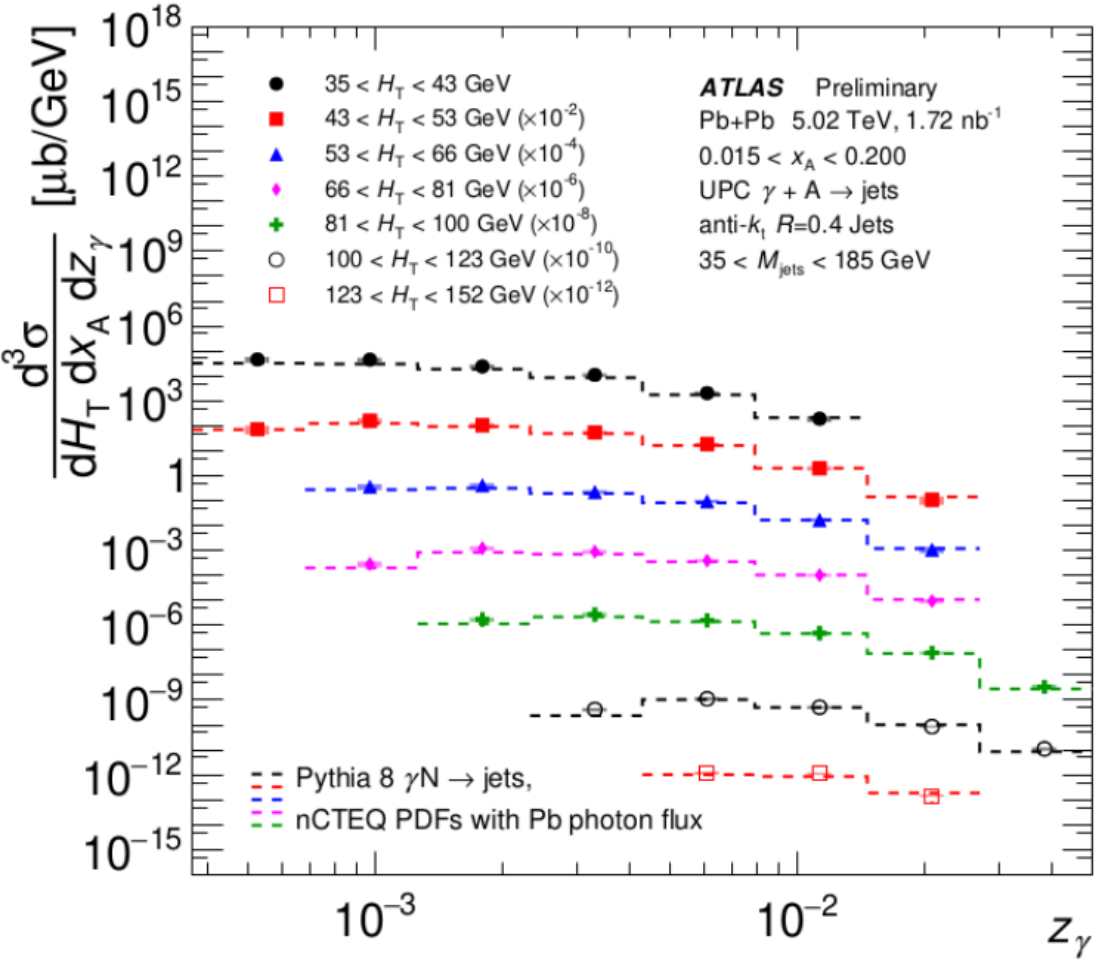

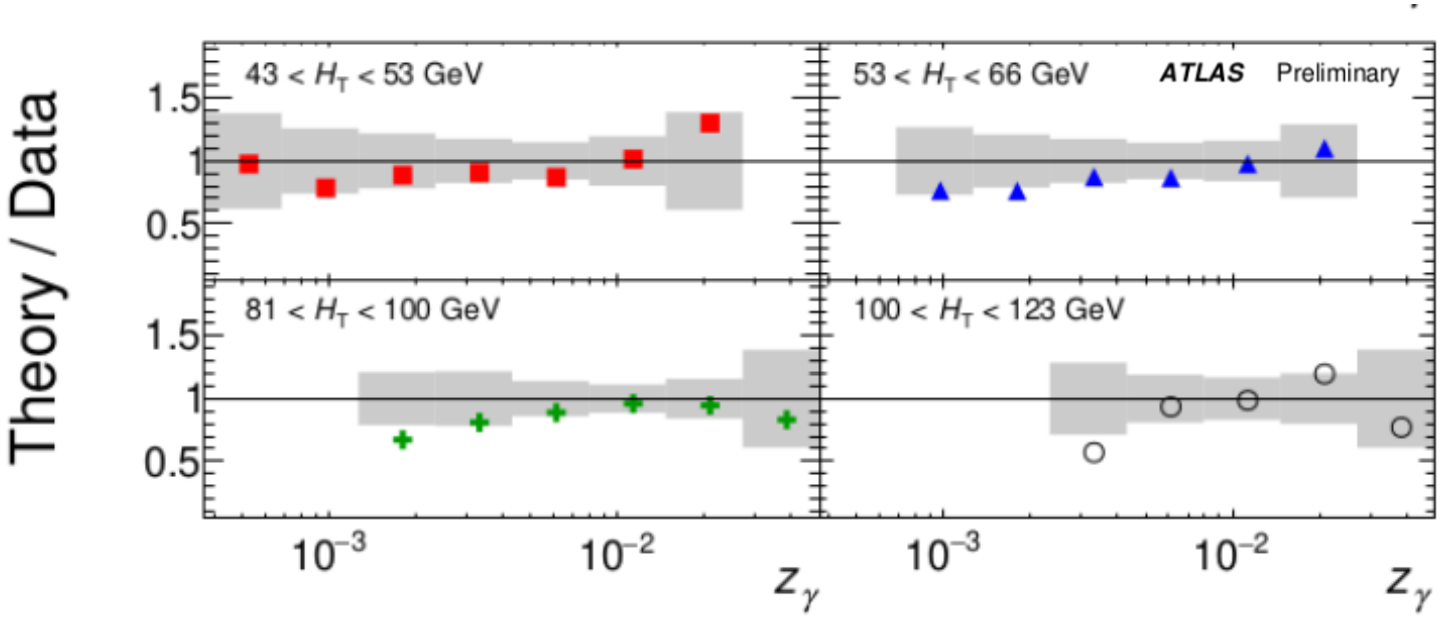

A comparison of data with the Pythia 8 distributions shows systematic differences which, combined with the disparity in yields may indicate contributions from processes not included in the Pythia 8 simulation.

Charged hadron yields in photonuclear collisions

ATLAS-CONF-2023-059

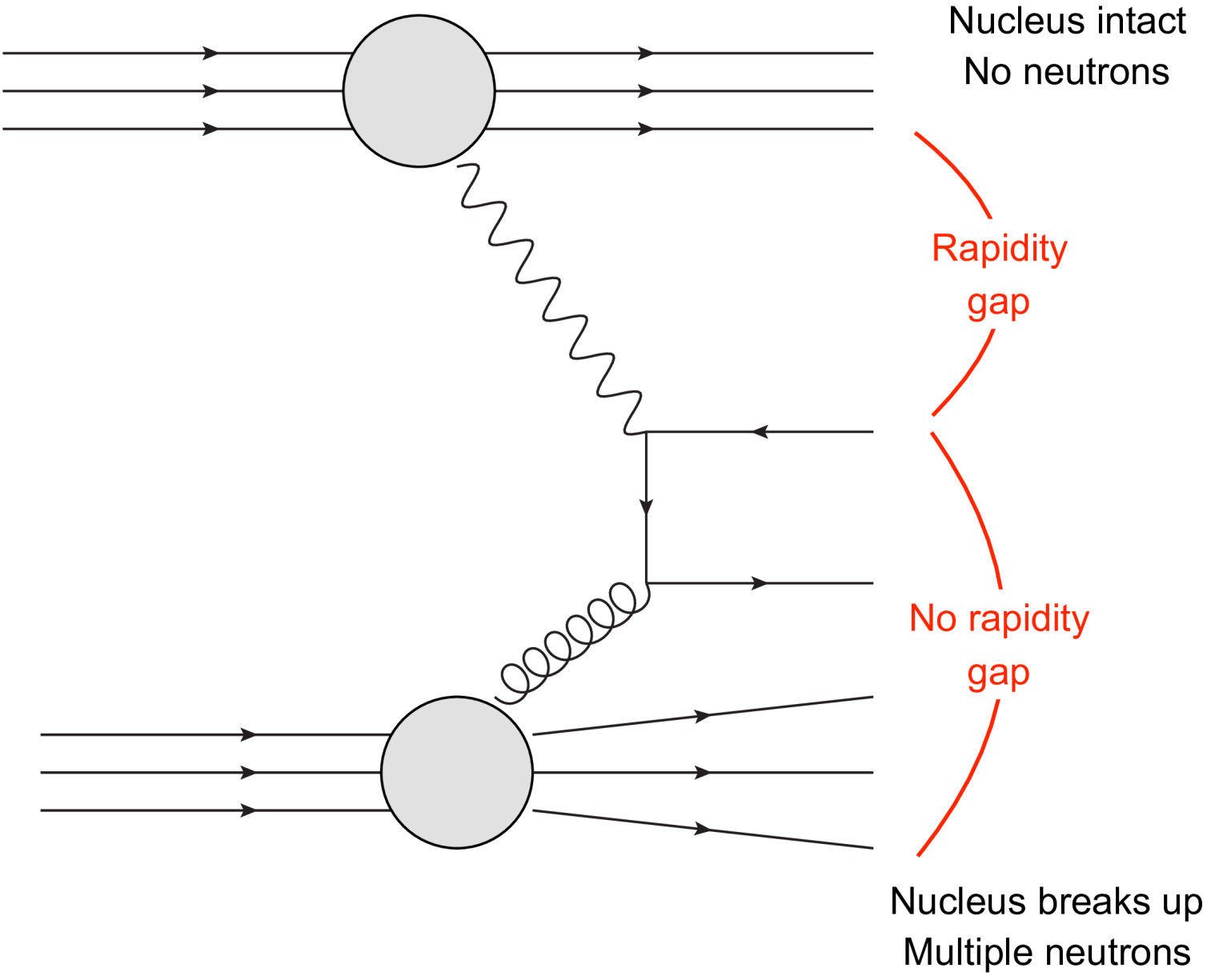

- photo-nuclear collisions
- 1.73 nb^{-1} of 5.02 TeV Pb+Pb collected in 2018
- 0.10 nb^{-1} of 5.02 TeV p+Pb data collected in 2016

Charged hadron yields in photonuclear collisions

ATLAS-CONF-2023-059

Multiplicity distribution (N_{ch}^{rec}) from Pb+Pb UPC (left) and *p*+Pb (right) collisions. N_{ch}^{rec} ranges, $25 < N_{ch}^{rec} \leq 60$, utilized in this analysis is highlighted.

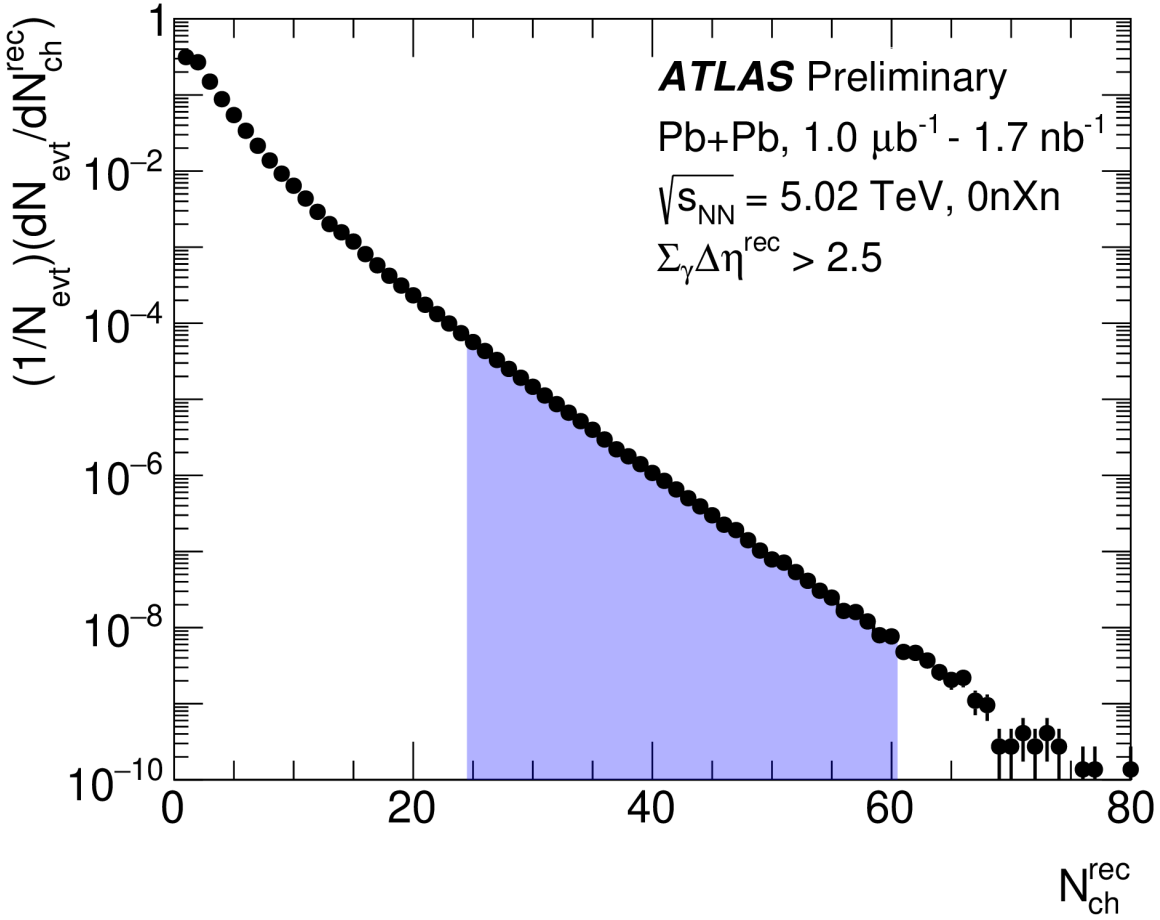

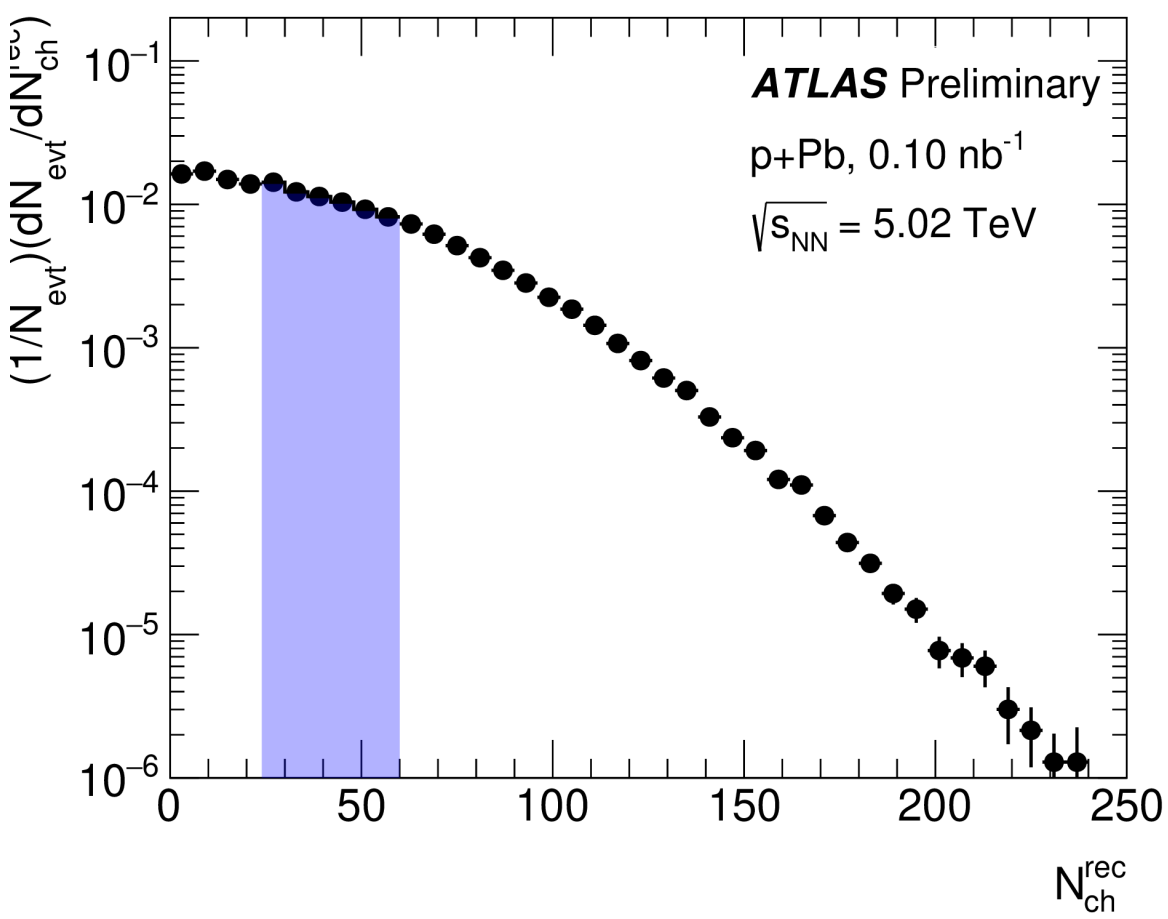

Charged hadron yields in photonuclear collisions

ATLAS-CONF-2023-059

Charged-hadron yields as a function of p_T in six η selections.
Left: UPC Pb+Pb collisions and the right: p+Pb collisions.

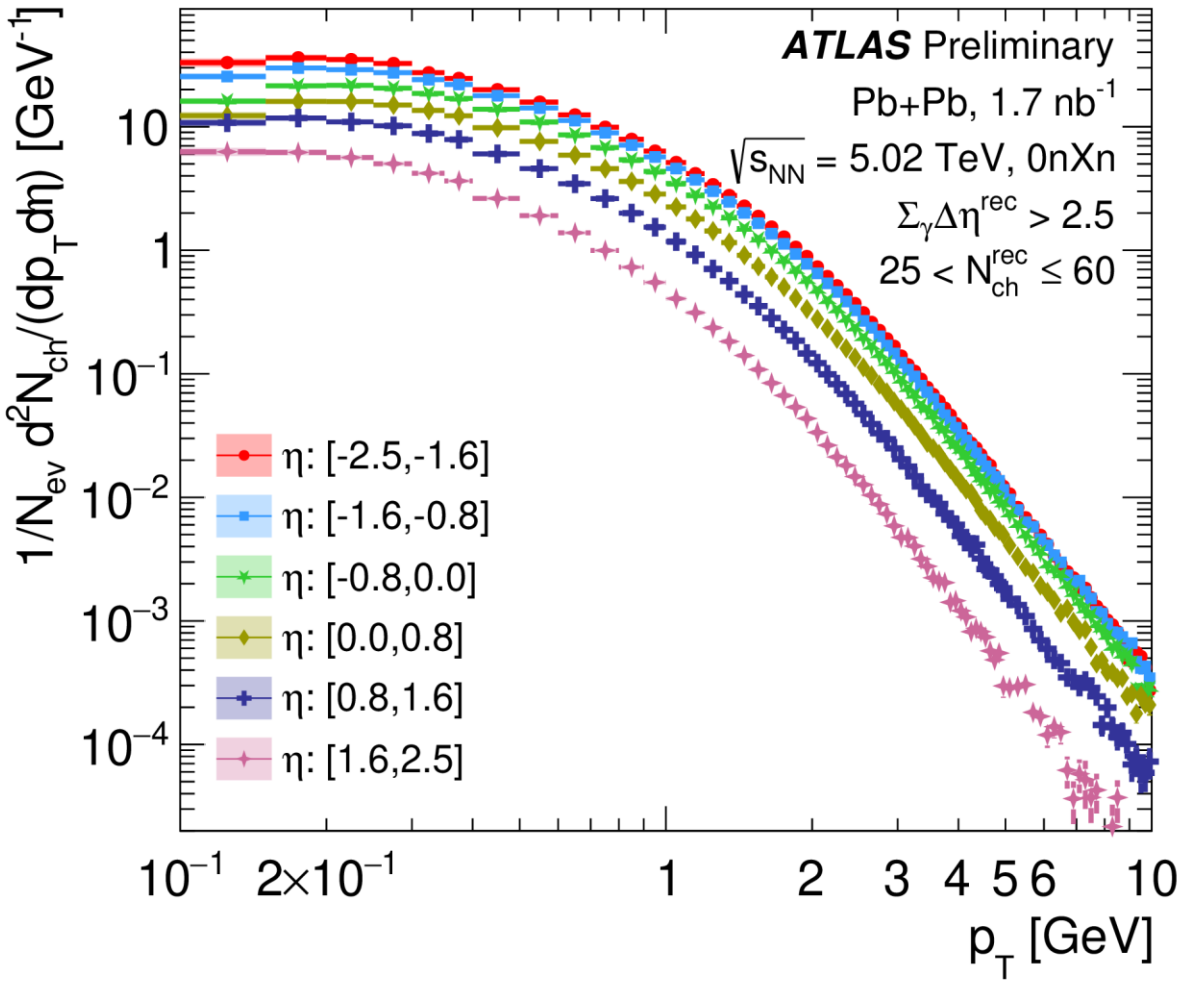

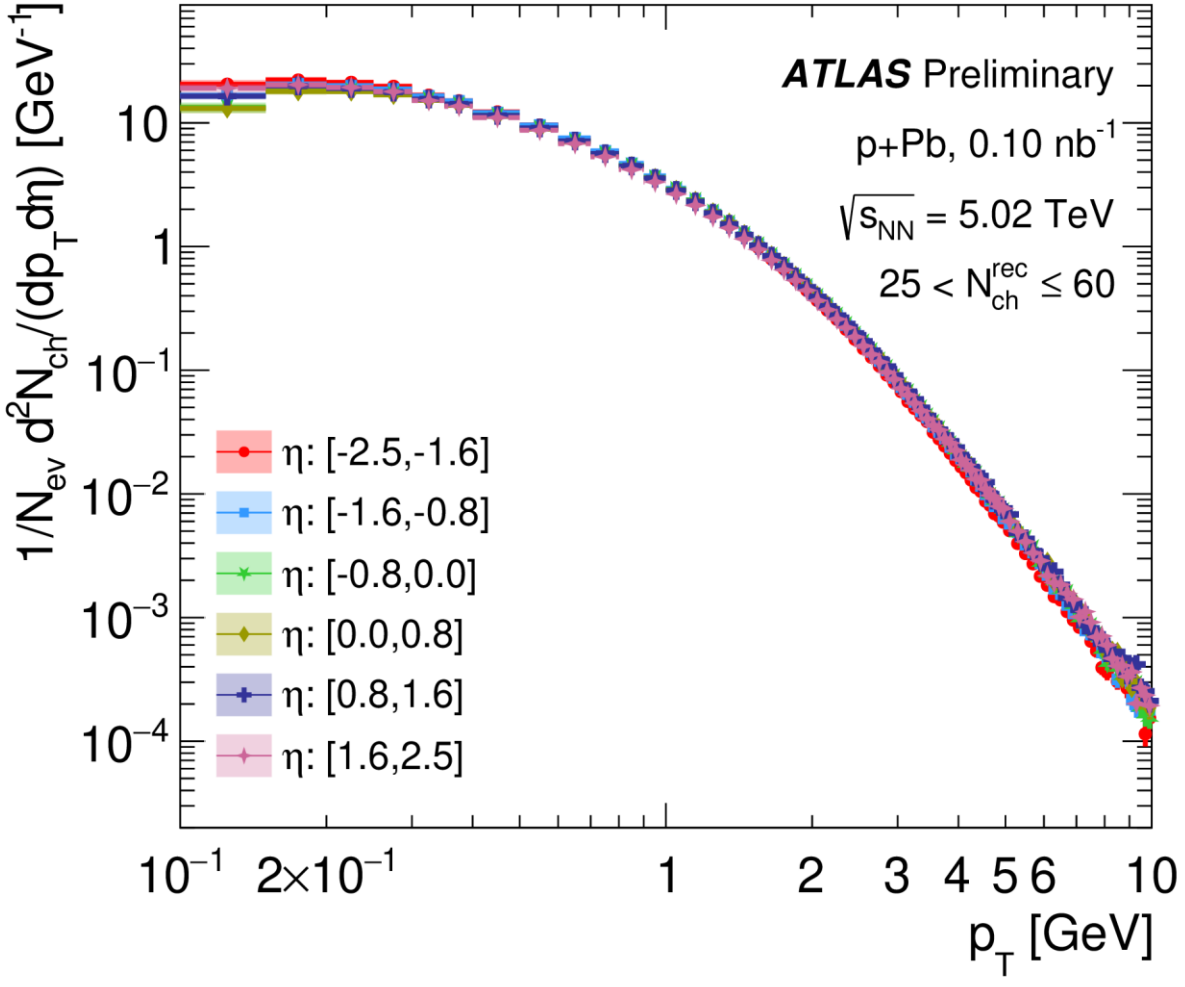

Charged hadron yields in photonuclear collisions

ATLAS-CONF-2023-059

Charged-hadron yields as a function of η extrapolated to $p_T > 0$ GeV for Pb+Pb UPC and p+Pb collisions

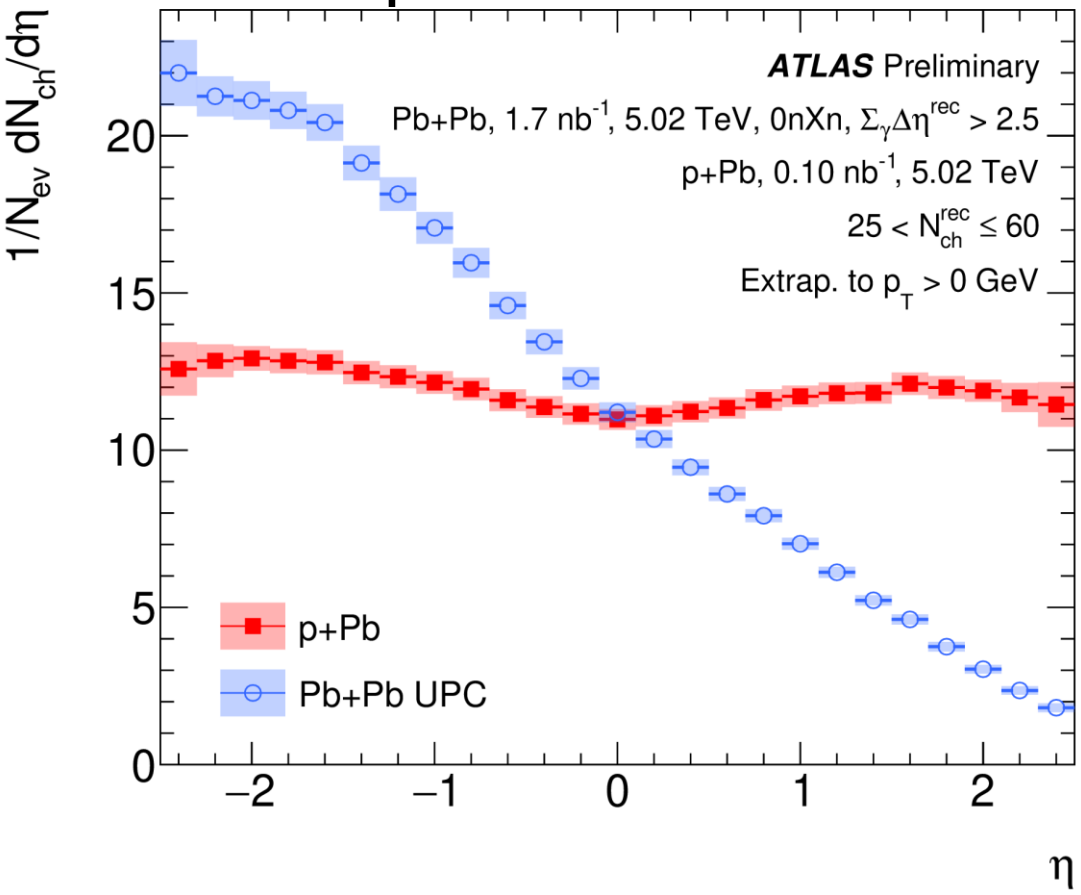

Truth-level yield result from reconstructed event generated by DPMJET-III utilizing the identical N_{ch}^{rec} and $\sum_\gamma \Delta\eta^{rec}$ selection criteria as with experimental Pb+Pb UPS data.

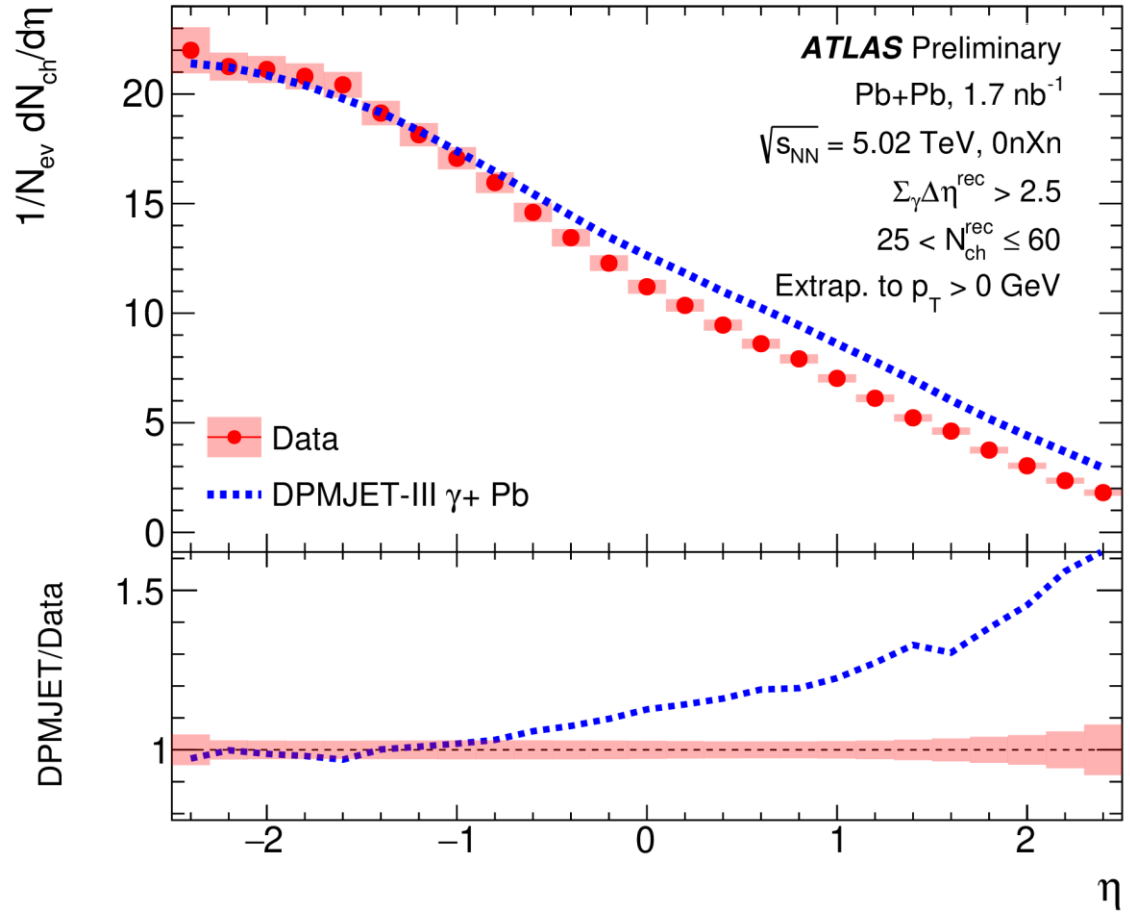

Observation of the $\gamma\gamma \rightarrow \tau\tau$ process and constraints on the tau-lepton anomalous magnetic moment

Phys. Rev. Lett. 131 (2023) 151802

Photon-induced τ-lepton pair production in UPV Pb+Pb interactions,

Pb+Pb → Pb(γγ→ ττ)Pb, with the τ-leptons decaying.

Left: one muon μ and one electron e.

Center: one muon and one charged pion $\pi^{\pm}$.

Right: one muon and three charged pions $\pi^{\pm}\pi^{\pm}\pi^{\pm}$.

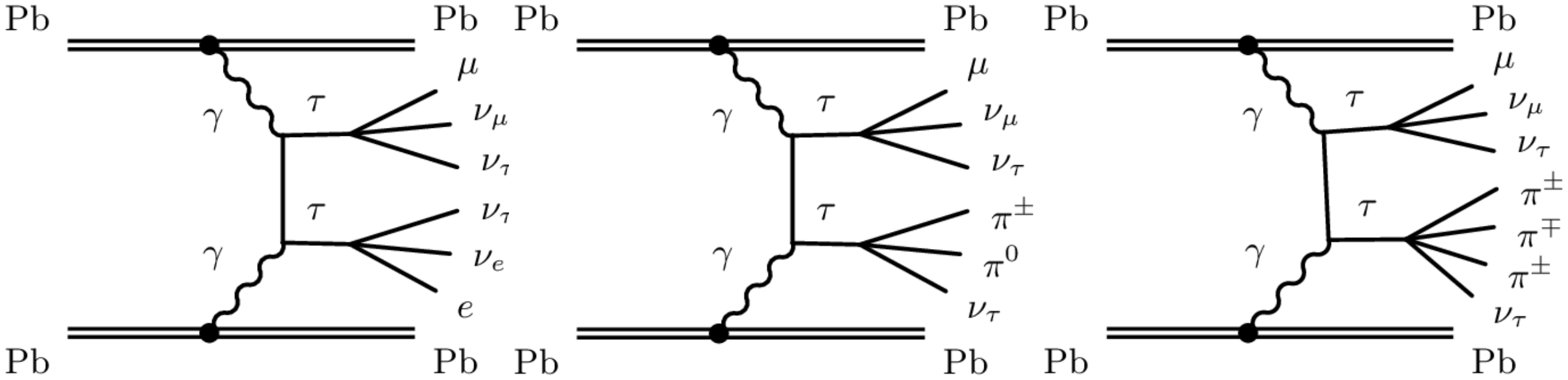

Observation of the $\gamma\gamma \rightarrow \tau\tau$ process and constraints on the tau-lepton anomalous magnetic moment

Phys. Rev. Lett. 131 (2023) 151802

Muon transverse momentum distributions.

Left: μe-SR. Center: μ1T-SR. Right: μ3T-SR.

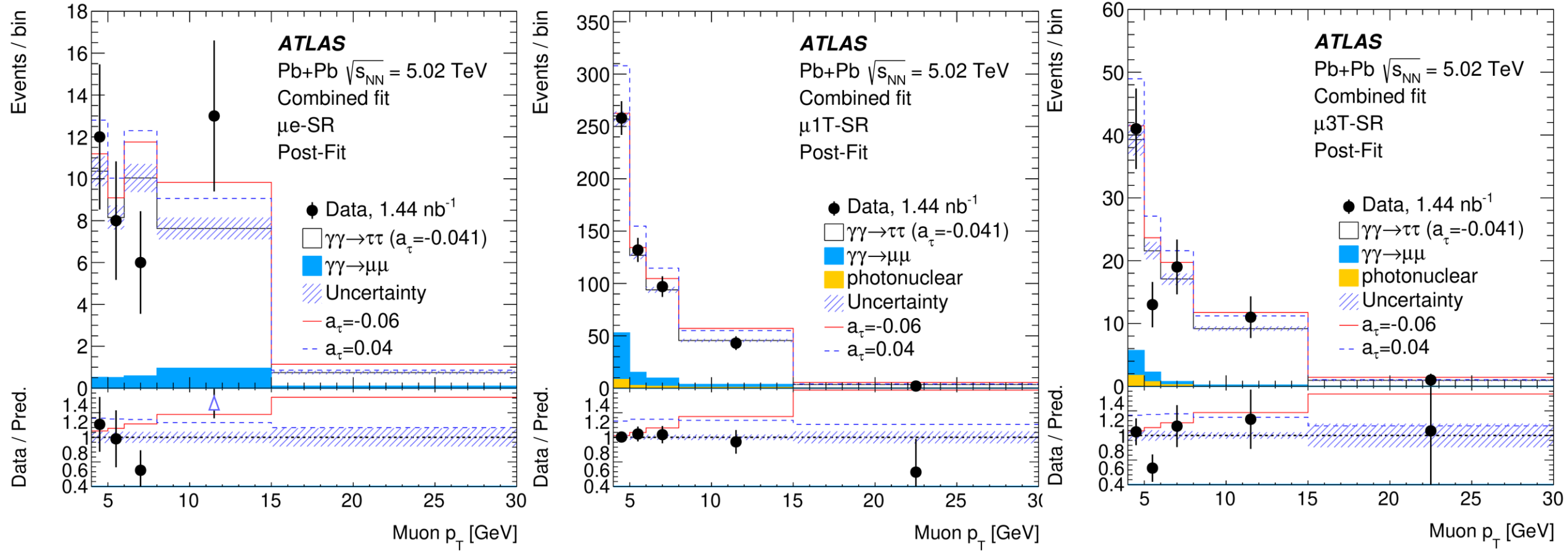

Observation of the $\gamma\gamma \rightarrow \tau\tau$ process and constraints on the tau-lepton anomalous magnetic moment

Phys. Rev. Lett. 131 (2023) 151802

Anomalous magnetic moment, $a_l = ½(g_l - 2)$ of charged leptons l (electrons, muons, and tau) are corner stone tests of the SM with unique sensitivity to BSM phenomena.

- $\gamma\gamma \rightarrow \tau\tau$ significance > 5 sd
- $\mu_{\tau\tau} = 1.03^{+0.06}_{-0.05}$ assuming SM value for a_τ
- Limit:
  $-0.057 < a_\tau < 0.024$
  at 95% CL

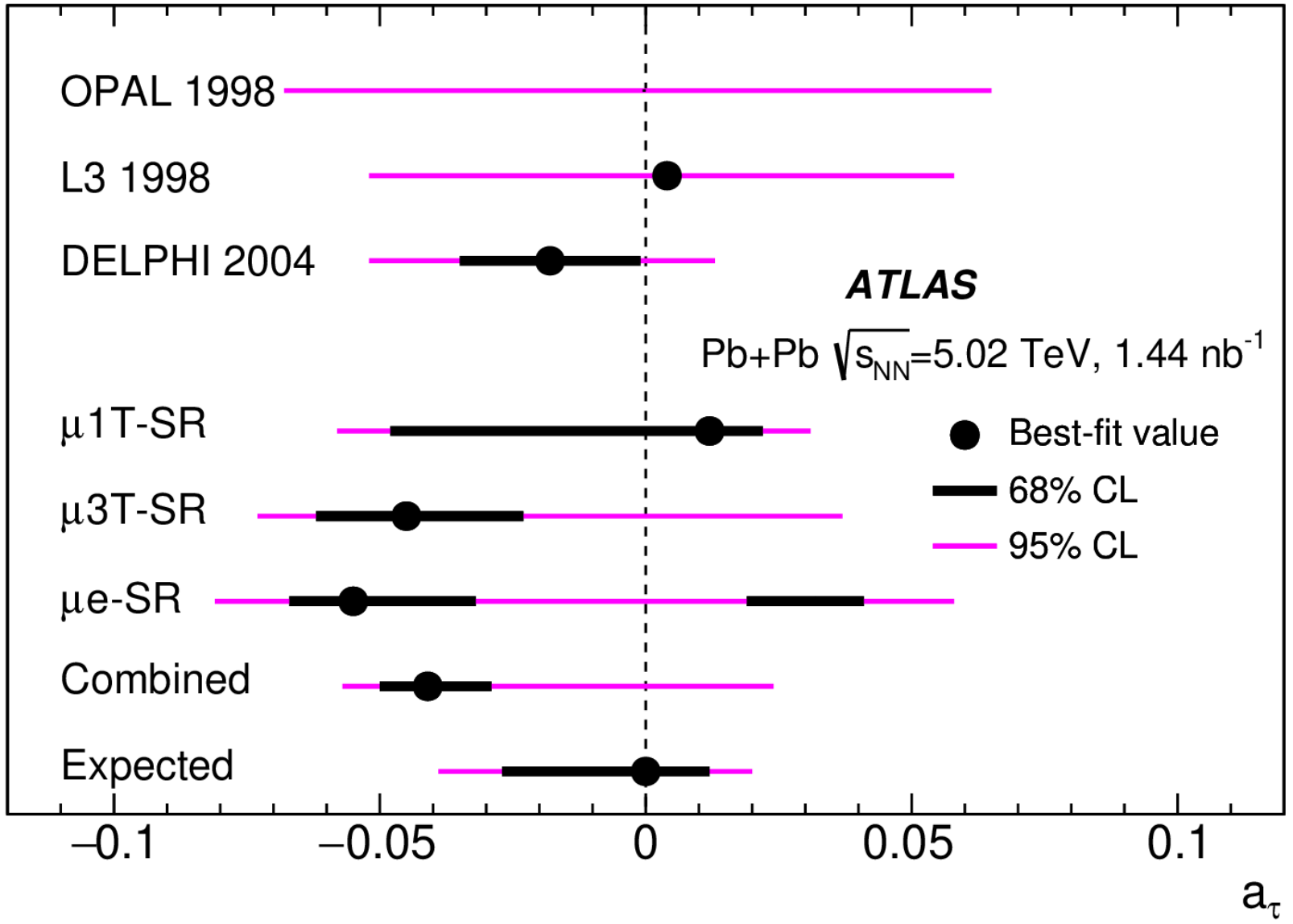

Search for magnetic monopoles in Pb+Pb UPC

2408.11035

- Pb+Pb UPC can be used to search for magnetic monopole pair production
- Occurs in strong magnetic fields, primarily via the Schwinger mechanism
- First search in Pb+Pb by MoEDAL, Nature 602 (2022) 63
- Large coupling of MM to photons → perturbation theory could not be used
- MM cross-section in HI UPC can be computed non-perturbatively using semiclassical models, e.g. Free-Particle-Approximation (FPA), arXiv:1902.04388:

$$\sigma_{FPA} = \frac{\omega}{m} \frac{2(q_m B)^4 R_{Pb}^4}{9\pi^2 m^4 \omega^2} \, exp(-4m/\omega)$$

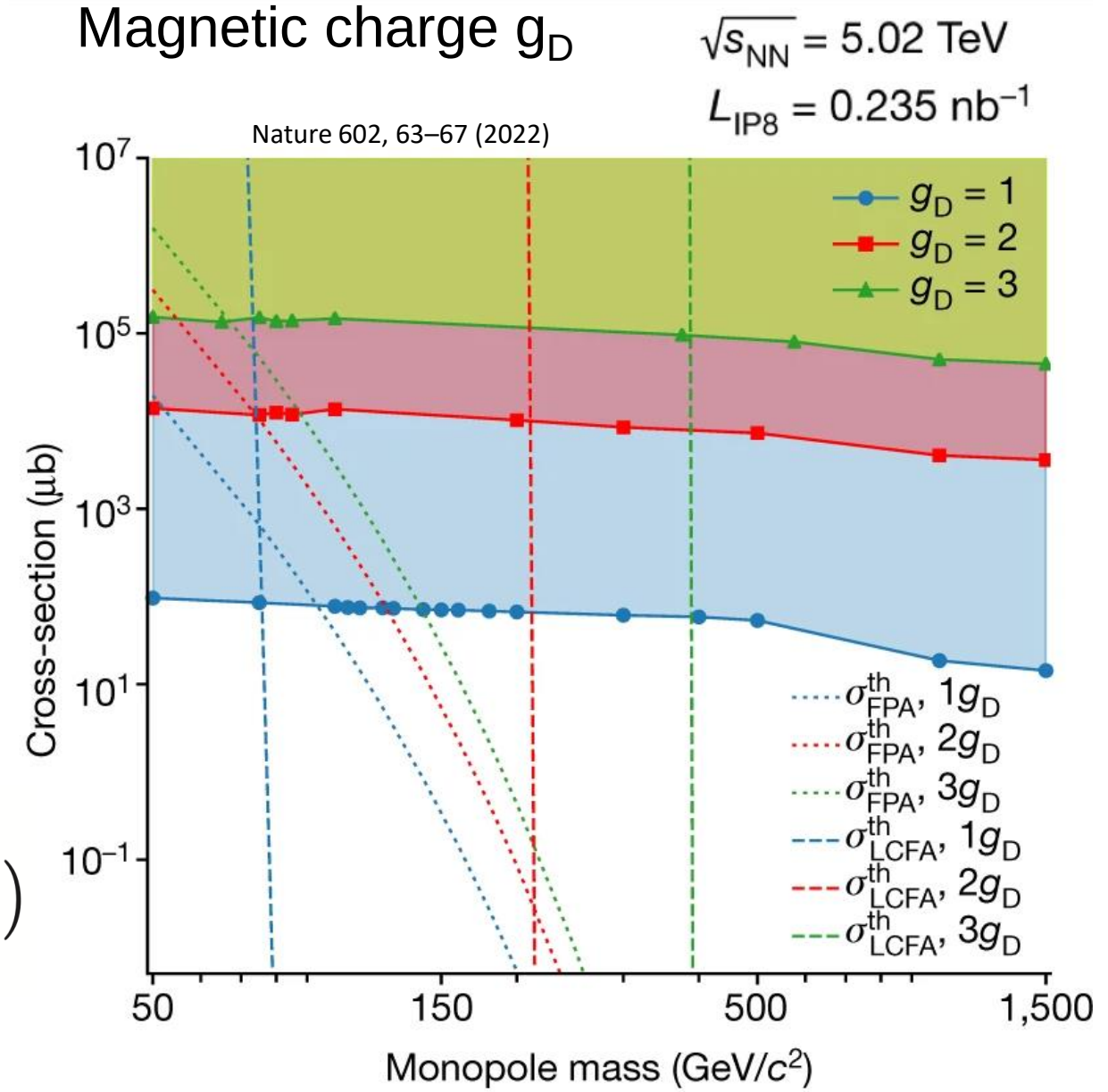

Search for magnetic monopoles in Pb+Pb UPC

2408.11035

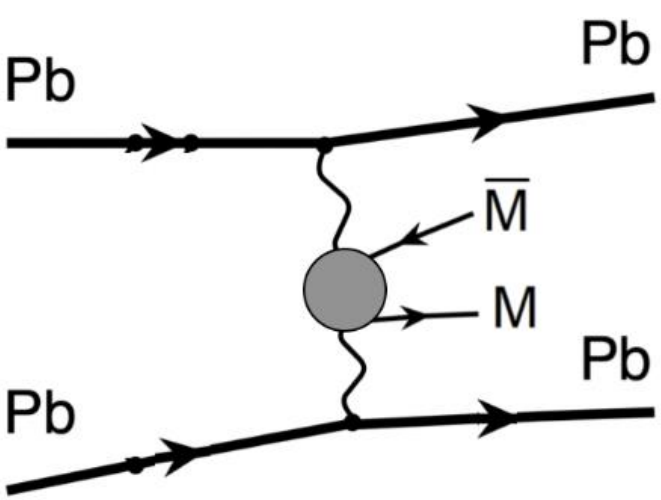

0n0n

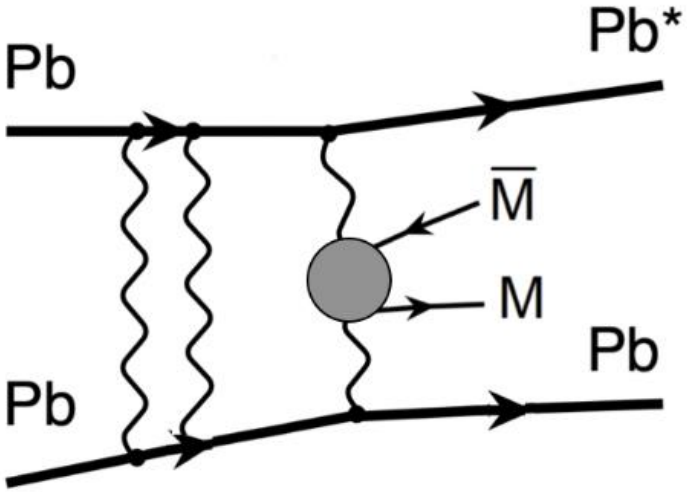

Xn0n

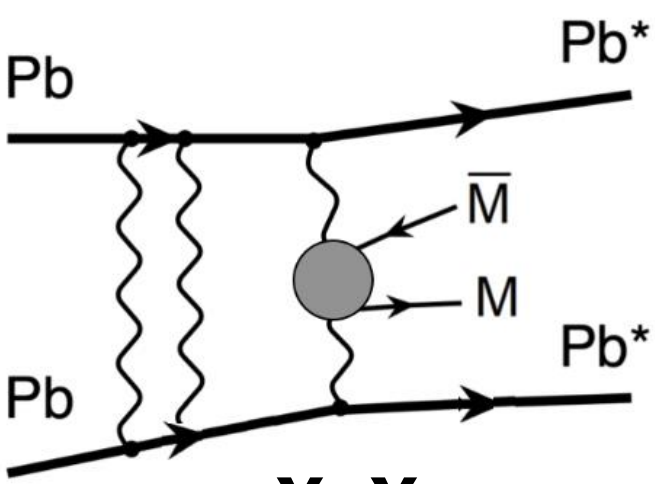

XnXn

Main signal category

- Different UPC topologies possible due to emission of neutrons
- Neutron detection with Zero Degree Calorimeters (ZDC)
- 2023 Pb+Pb data at $\sqrt{s_{NN}}$ = 5.36 TeV, 1.6 nb^{-1}, LHC Run-3 Pb+Pb data 2023
- Signal trigger:
  - L1: presence one or more neutrons in both ZDCs, and total ET < 10 GeV in calorimeter
  - HLT: presence of more than 100 Pixel clusters
  - Prescale: about 1/6 of events saved → 0.262 nb^{-1}

Search for magnetic monopoles in Pb+Pb UPC

2408.11035

Signal region definition:
transverse thrust T > 0.95

$$T = \frac{1}{n_{PixCL}} \sum_{i=i}^{n_{PixCL}} |\hat{r}_i \cdot \hat{n}|$$

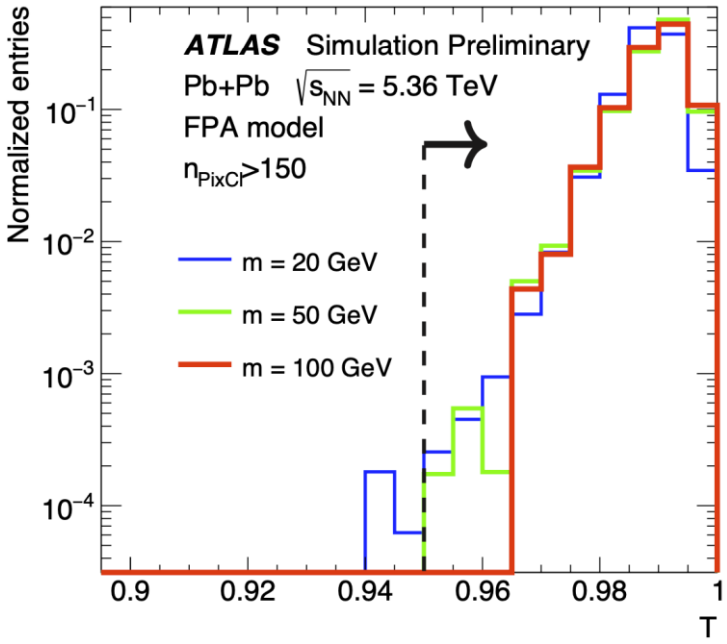

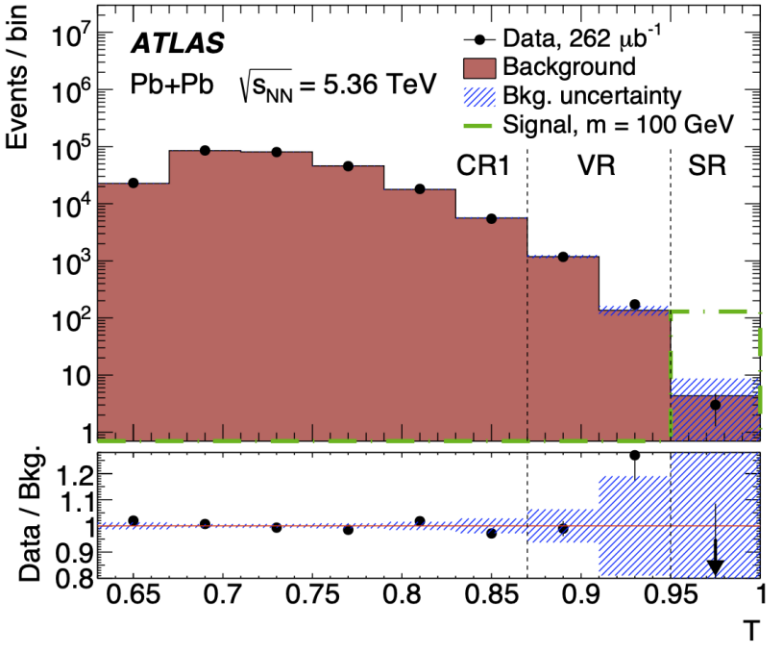

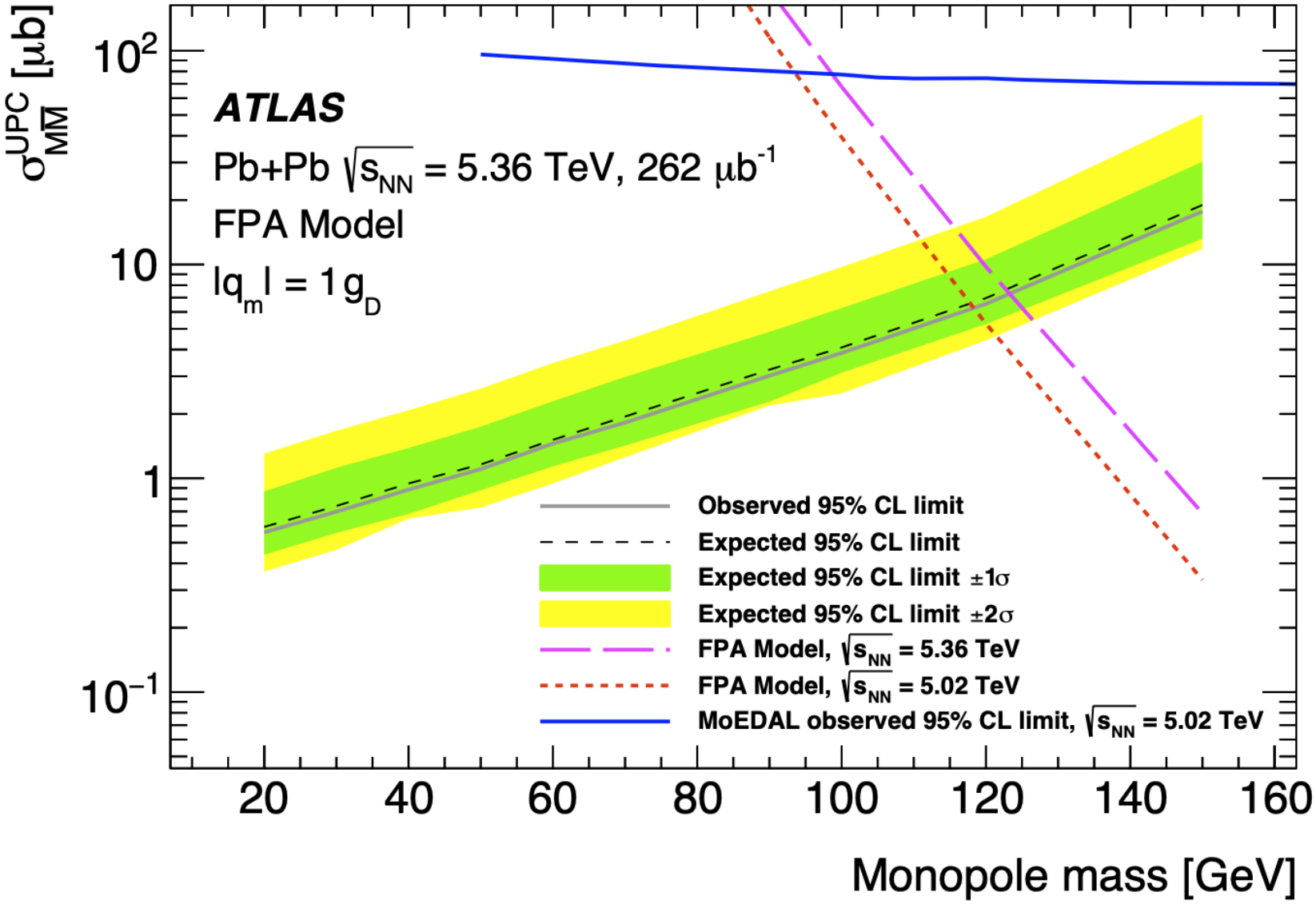

Electroweak, QCD and flavour physics studies
Observation of photon-induced WW production

2404.06829

Phys. Lett. B 816 (2021) 136190

- Proton-proton collisions at 13 TeV, 139 fb^{-1}
- Di-boson system final state $\gamma\gamma \rightarrow WW \rightarrow e\mu$

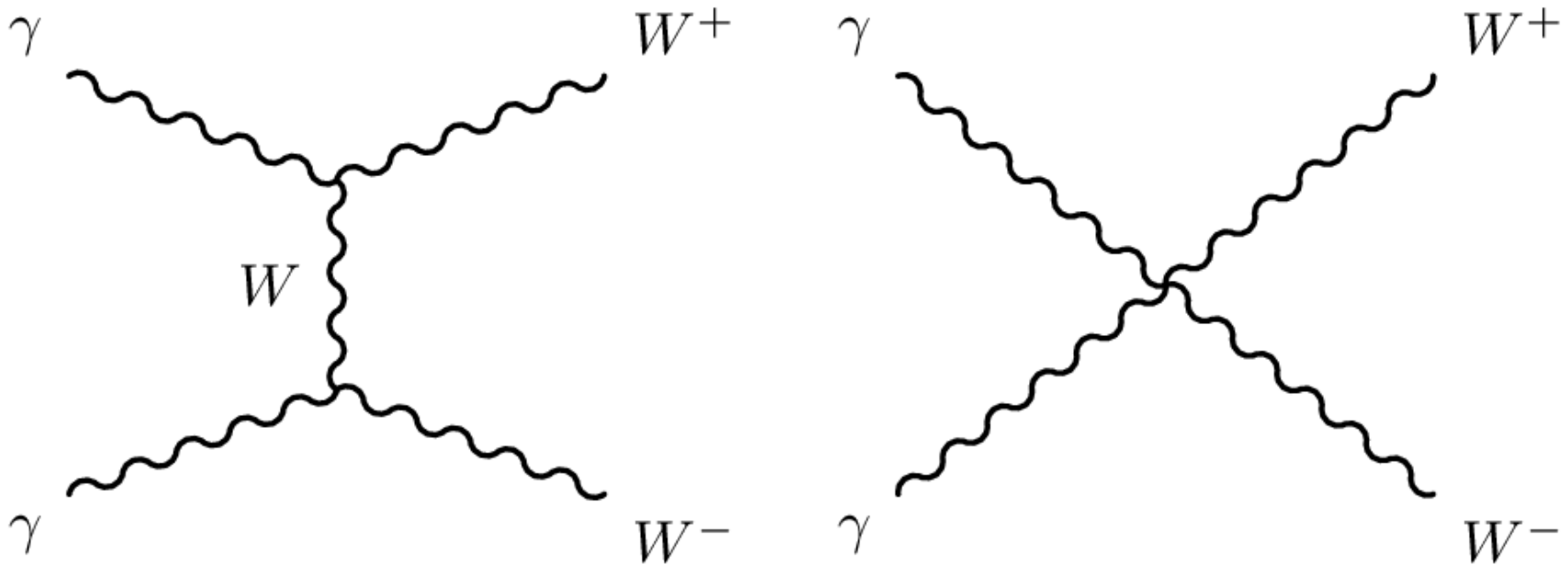

Electroweak, QCD and flavour physics studies
Observation of photon-induced WW production

2404.06829

Phys. Lett. B 816 (2021) 136190

- Normalised distribution of tracks from additional pp interactions, n^{PU}_{trk}, associated with the interaction vertex, in data and signal simulated with a beam spot width of σ^{BS}_{MC}**= 42 mm**.
- For data, n^{PU}_{trk} is determined using a random z-position along the beam axis away from the interaction vertex.
- Simulation with GEANT4 without and with beam spot width correction.
- $\gamma\gamma \rightarrow WW \rightarrow e\mu$ simulation with correction

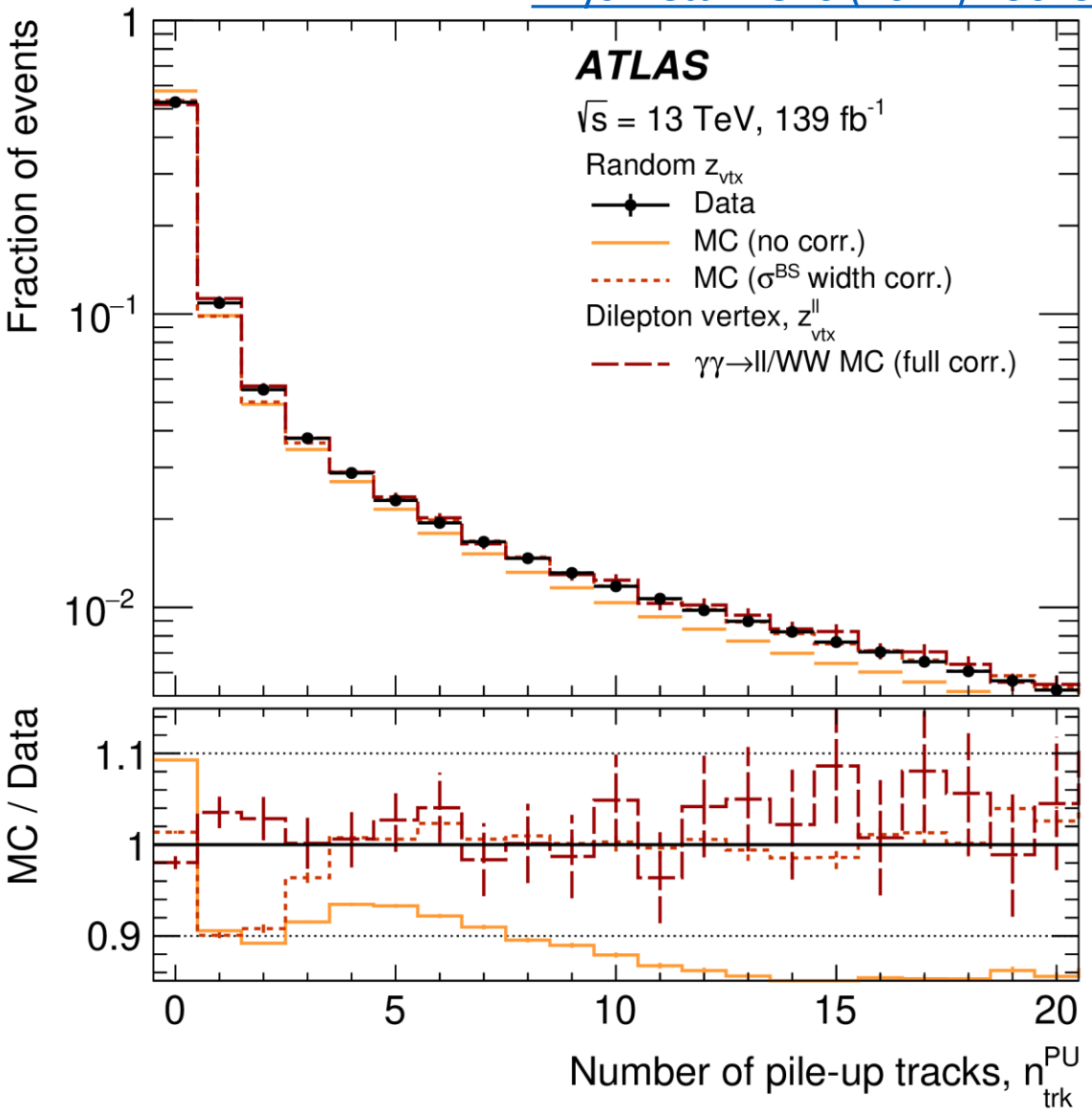

Electroweak, QCD and flavour physics studies
Observation of photon-induced WW production

2404.06829

Phys. Lett. B 816 (2021) 136190

- $p_T^{e\mu}$ for n_{track}=0
- Drell-Yan background at low $p_T^{e\mu}$
- Require $p_T^{e\mu}$ >30 GeV
- Some remaining background from $qq \rightarrow WW \rightarrow e\mu$

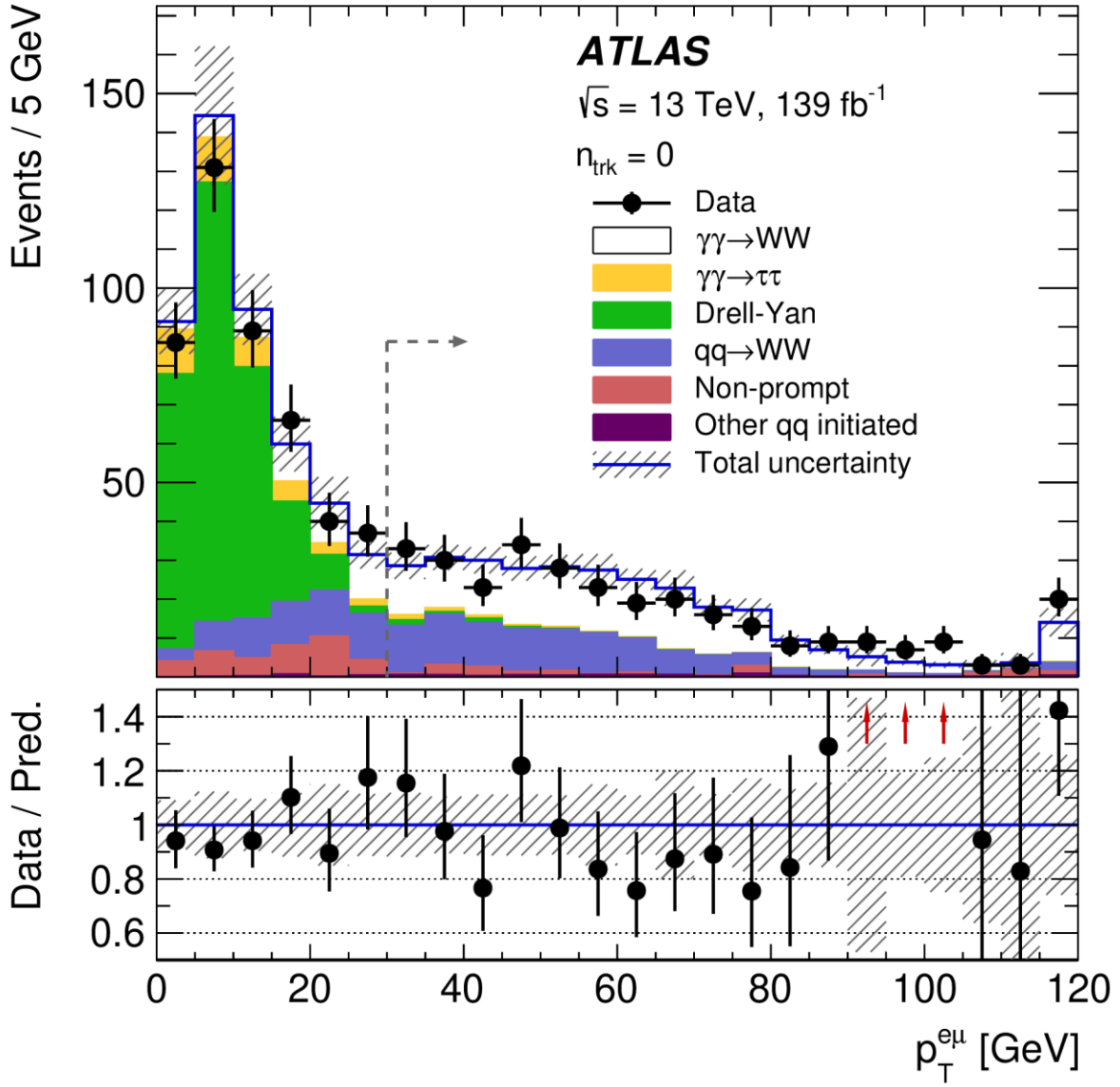

Electroweak, QCD and flavour physics studies
Observation of photon-induced WW production

2404.06829

Phys. Lett. B 816 (2021) 136190

- number of tracks associated with the interaction vertex
- $\gamma\gamma \rightarrow WW$ signal region requires a selection of $n_{track}=0$
- $qq \rightarrow WW$ component also contains a small contribution from gluon-induced WW and electroweak WWjj production
- "other qq initiated" includes contributions not only from WZ and ZZ diboson production but also from top-quark production and other gluon-induced processes

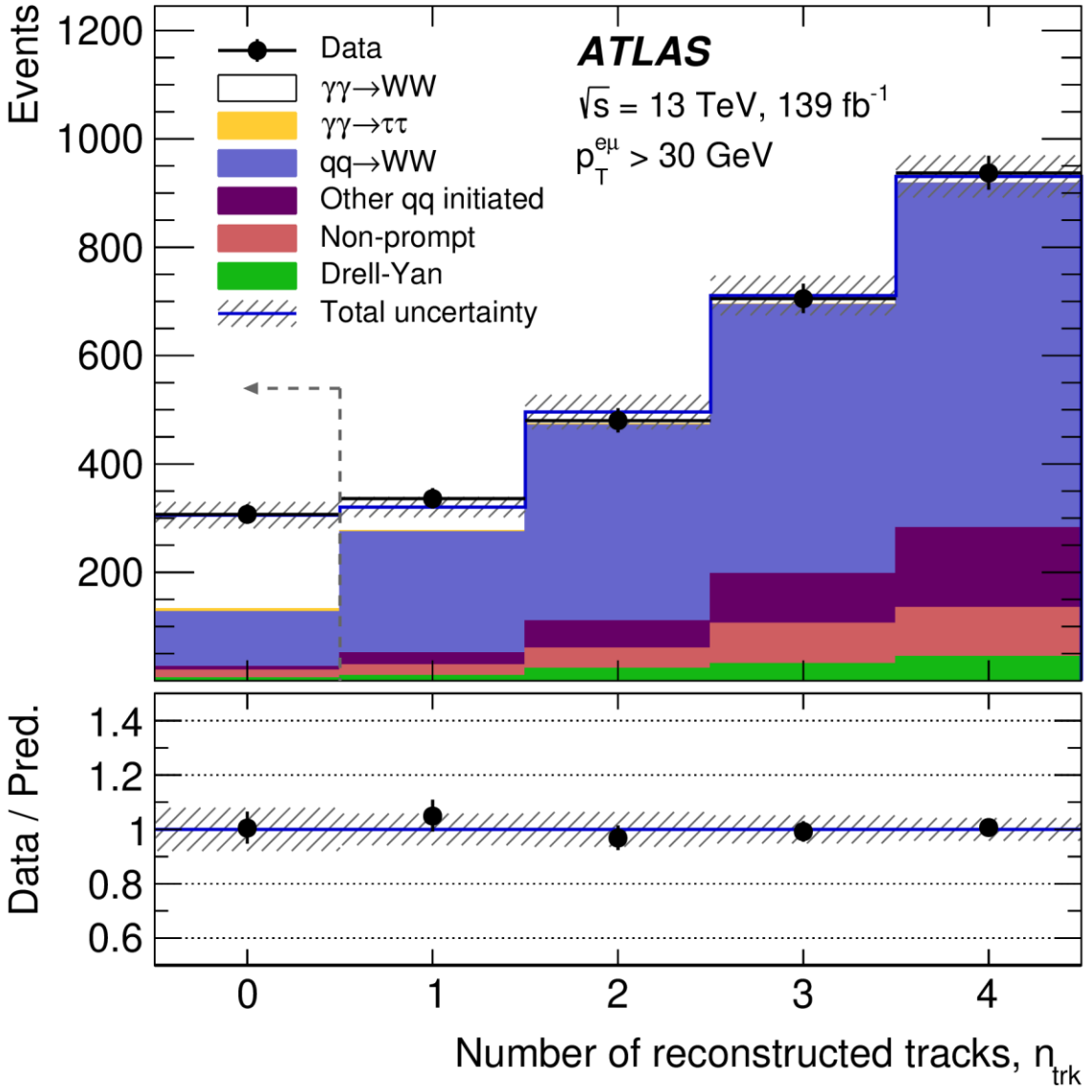

Electroweak, QCD and flavour physics studies
Observation of photon-induced WW production

2404.06829

Phys. Lett. B 816 (2021) 136190

	Signal region		Control regions	
n_{trk}	$n_{\text{trk}} = 0$		$1 \leq n_{\text{trk}} \leq 4$	
$p_{\text{T}}^{e\mu}$	> 30 GeV	< 30 GeV	> 30 GeV	< 30 GeV
$\gamma\gamma \to WW$	174 ± 20	45 ± 6	95 ± 19	24 ± 5
$\gamma\gamma \to \ell\ell$	5.5 ± 0.3	39.6 ± 1.9	5.6 ± 1.2	32 ± 7
Drell–Yan	4.5 ± 0.9	280 ± 40	106 ± 19	4700 ± 400
$qq \to WW$ (incl. gg and VBS)	101 ± 17	55 ± 10	1700 ± 270	970 ± 150
Non-prompt	14 ± 14	36 ± 35	220 ± 220	500 ± 400
Other backgrounds	7.1 ± 1.7	1.9 ± 0.4	311 ± 76	81 ± 15
Total	305 ± 18	459 ± 19	2460 ± 60	6320 ± 130
Data	307	449	2458	6332

Electroweak, QCD and flavour physics studies
Observation of photon-induced WW production

2404.06829

Phys. Lett. B 816 (2021) 136190

- **Cross-section $\sigma(\gamma\gamma \rightarrow WW)$** =3.13 ±0.31 (stat.) ±0.28 (syst.) fb
- Significance 8.4 sd

Source of uncertainty	Impact [% of the fitted cross section]
Experimental	
Track reconstruction	1.1
Electron energy scale and resolution, and efficiency	0.4
Muon momentum scale and resolution, and efficiency	0.5
Misidentified leptons, systematic	1.5
Misidentified leptons, statistical	5.9
Other background, statistical	3.2
Modelling	
Pile-up modelling	1.1
Underlying-event modelling	1.4
Signal modelling	2.1
WW modelling	4.0
Other background modelling	1.7
Luminosity	1.7
Total	8.9

Observation of forward proton scattering in association with lepton pairs produced in photon fusion

Phys. Rev. Lett. 125 (2020) 261801

- **Scattered protons detected by ATLAS Forward Proton (AFP) spectrometer**
- **Light leptons (ee or $\mu\mu$) reconstructed in ATLAS central detector**

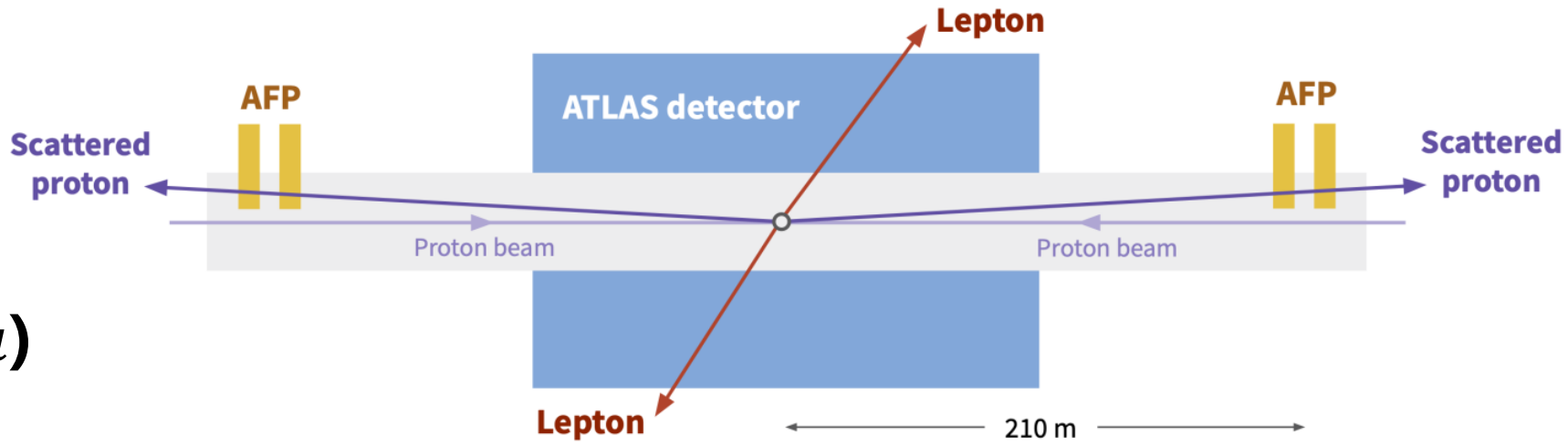

- **Signal: exclusive or single dissociative (soft QCD) and re-scattering**

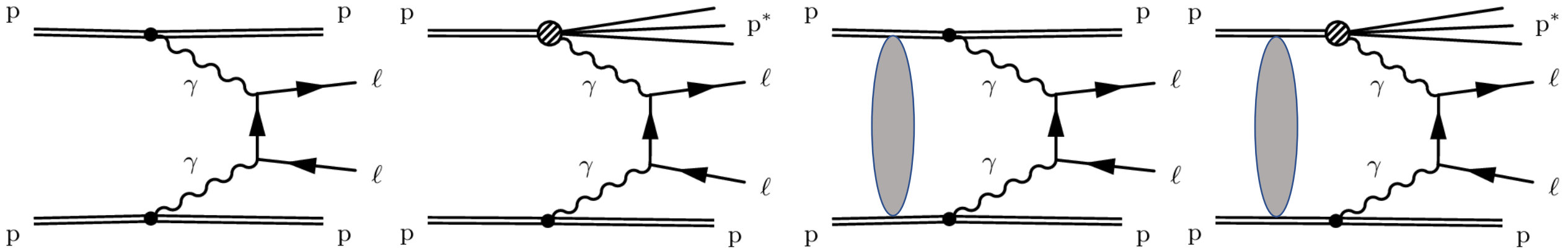

Observation of forward proton scattering in association with lepton pairs produced in photon fusion

Phys. Rev. Lett. 125 (2020) 261801

- matching of lepton pair and proton kinematics, ξ_{ll}, ξ_{AFP}
- AFP detection range $0.02 < \xi < 0.12$
- Signal and combinatorial background processes
- p^* dissociated proton

$$\xi_{ll} = (m_{ll}/\sqrt{s})e^{\pm y_{ll}}, \quad \xi_{AFP} = 1 - E_p/E_{beam}$$

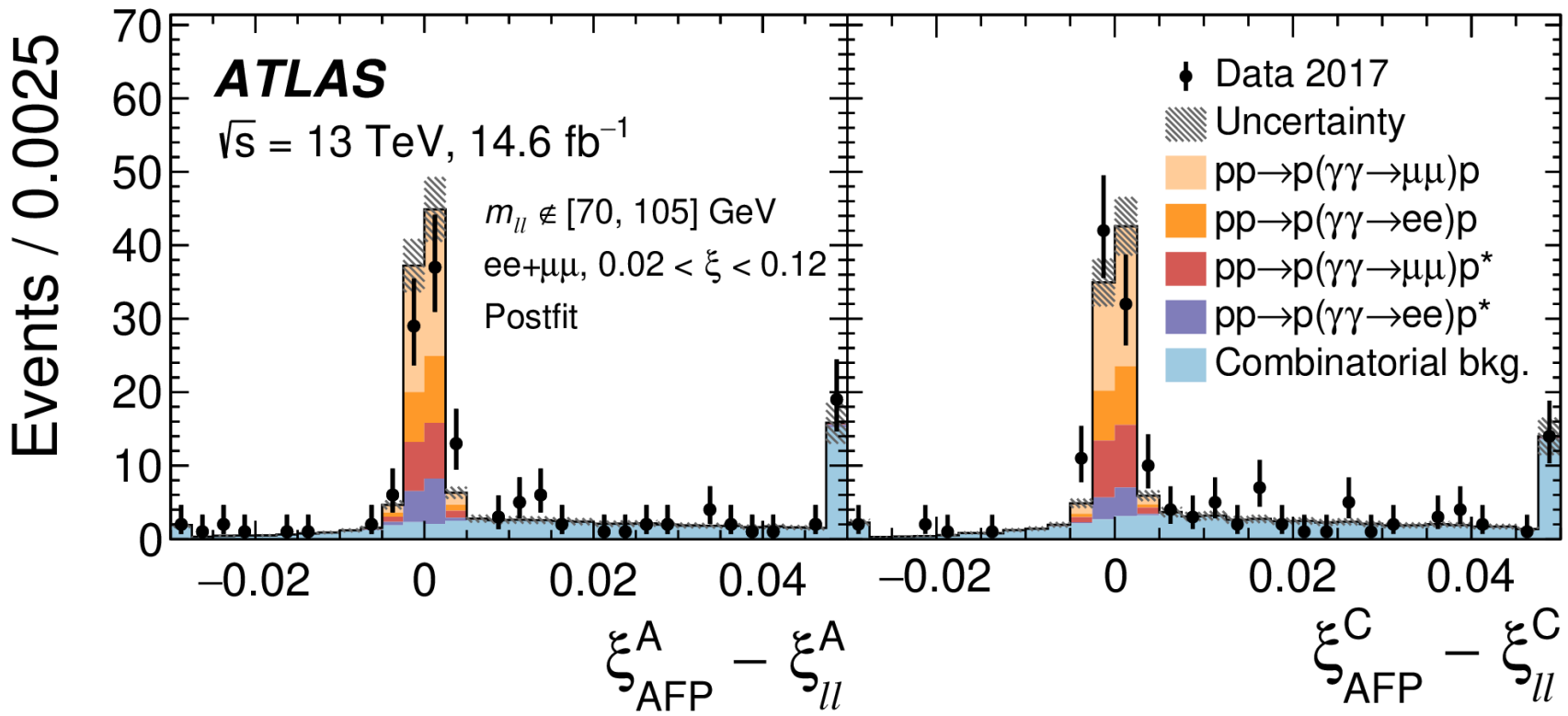

Observation of forward proton scattering in association with lepton pairs produced in photon fusion

Phys. Rev. Lett. 125 (2020) 261801

- Data event candidates: dilepton rapidity $y_{\ell\ell}$ versus $m_{\ell\ell}$ plane
- Event selection and kinematic matching $|\xi_{AFP} - \xi_{\ell\ell}| < 0.005$ on at least one side
- Shaded (hatched) areas denote the acceptance (no acceptance) for the AFP stations
- Areas neither shaded nor hatched correspond to $\xi \notin [0, 1]$
- Future double tag events will increase distinction between exclusive/dissociated production

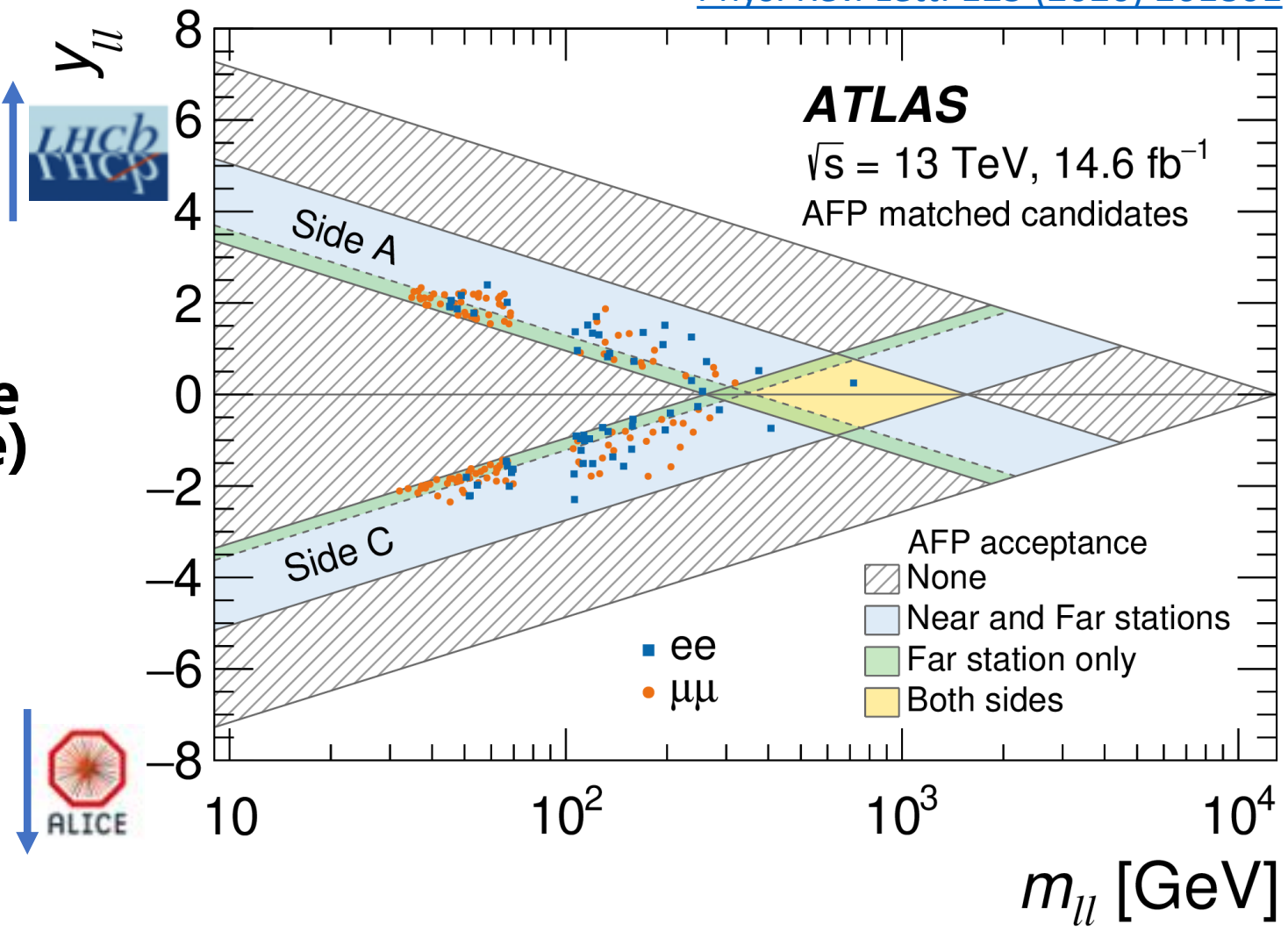

Observation of forward proton scattering in association with lepton pairs produced in photon fusion

Phys. Rev. Lett. 125 (2020) 261801

- **57 (123) candidates in the e^+e^-+p ($\mu^+\mu^-$+p) final states**
- **Background-only hypothesis rejected with a significance >5σ in each channel**
- **Cross-section measurements in the fiducial detector acceptance $\xi \in$[0.035; 0.08]**

σ(ee+p) = 11.0 $\pm$2.6 (stat) $\pm$1.2 (syst) $\pm$0.3 (lumi) fb

$\sigma(\mu\mu$+p) = 7.2 $\pm$1.6 (stat) $\pm$0.9 (syst) $\pm$0.3 (lumi) fb

- **Comparison with proton soft survival (no additional soft re-scattering) models:**

$\sigma_{\text{HERWIG+LPAIR}} \times S_{\text{surv}}$	$\sigma^{\text{fid.}}_{ee+p}$ [fb]	$\sigma^{\text{fid.}}_{\mu\mu+p}$ [fb]
$S_{\text{surv}} = 1$	15.5 ± 1.2	13.5 ± 1.1
S_{surv} using Refs. [31,30]	10.9 ± 0.8	9.4 ± 0.7
SUPERCHIC 4 [94]	12.2 ± 0.9	10.4 ± 0.7
Measurement	11.0 ± 2.9	7.2 ± 1.8

[31] Eur. Phys. J. C 76 (2016) 9
[30] Phys. Lett. B 741 (2015) 66
[94] Eur. Phys. J. C80 (2020) 925

Di-photon resonance search with AFP tag

JHEP 07 (2023) 234

In the $\gamma\gamma \to \gamma\gamma$ event, final state proton can be intact (not dissociative)

Exclusive event

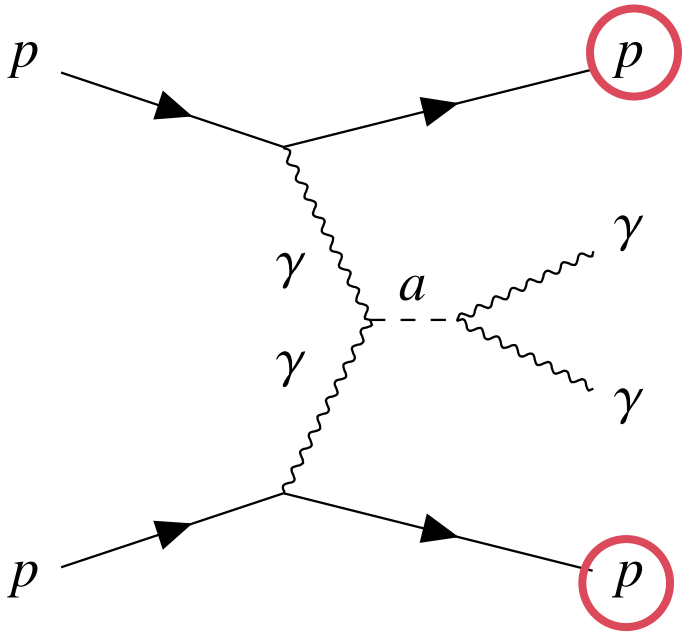

Single-dissociative (SD) event

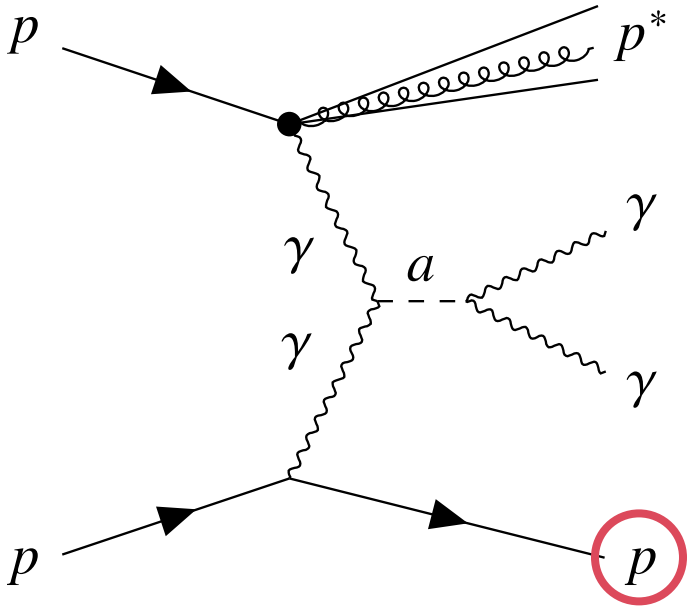

Double-dissociative (DD) event

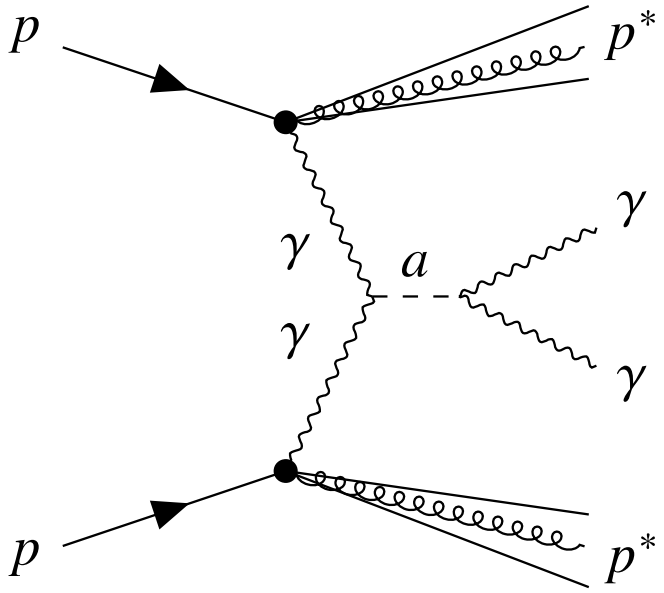

ALP Production Cross-section

JHEP 07 (2023) 234

Coupling constant
f^{-1}=0.05 TeV^{-1}

SuperChic 4.02
for EL
SuperChic 4.14
for SD and DD

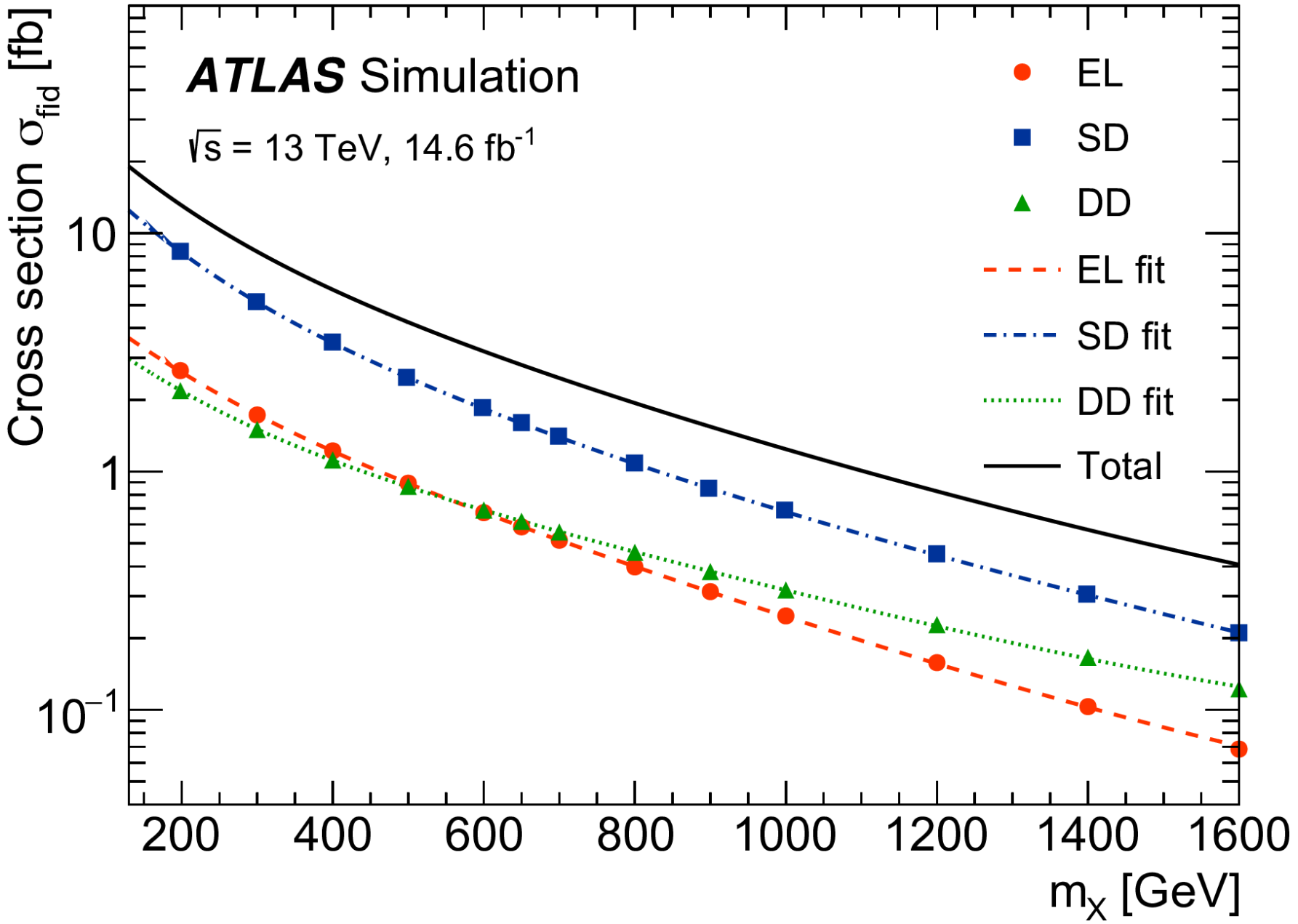

Signal Yields

JHEP 07 (2023) 234

Coupling constant
$f^{-1}=0.05\ TeV^{-1}$

signal efficiency ×
acceptance models ×
cross-section ×
luminosity

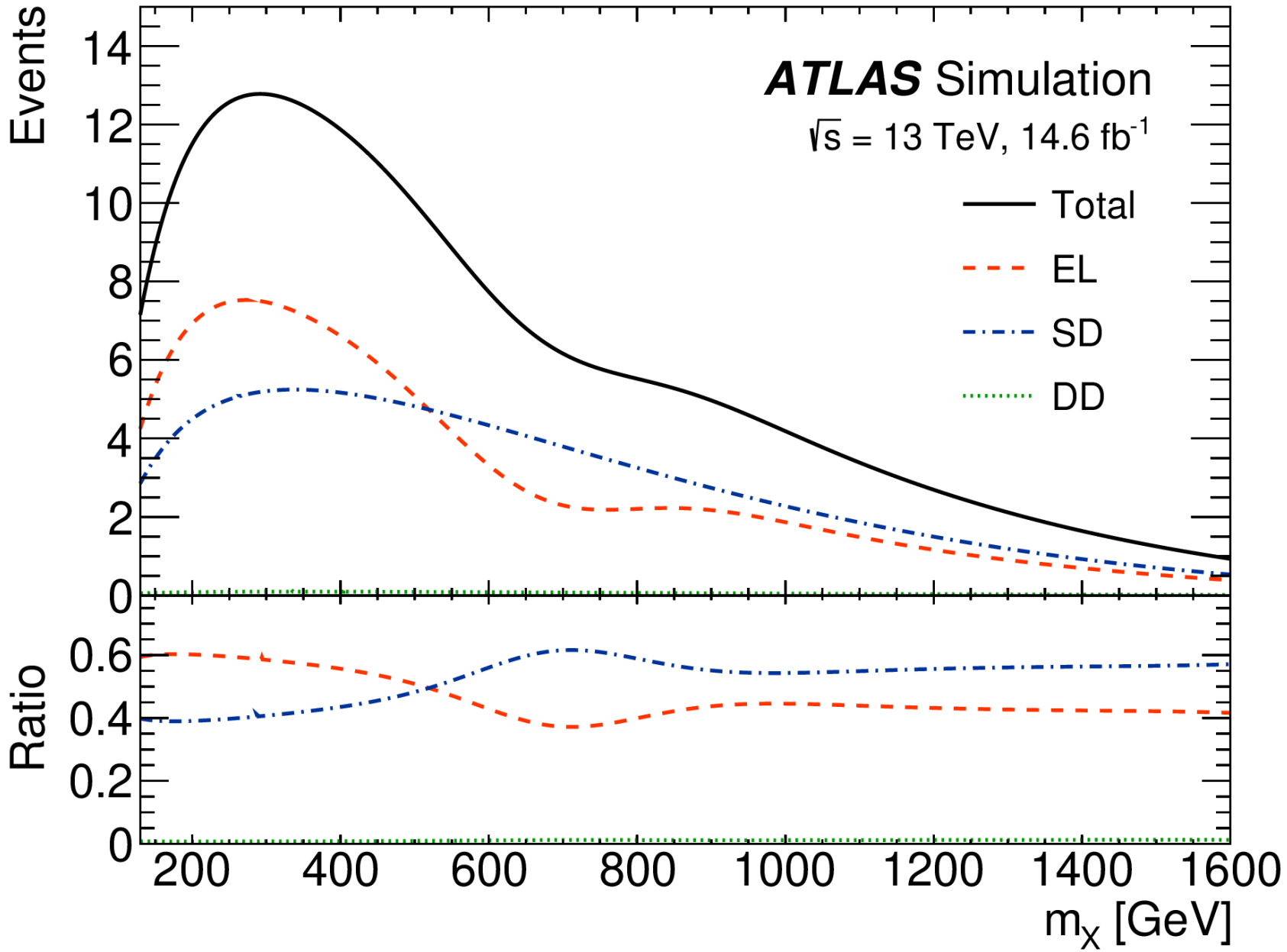

Data and background-only fit

JHEP 07 (2023) 234

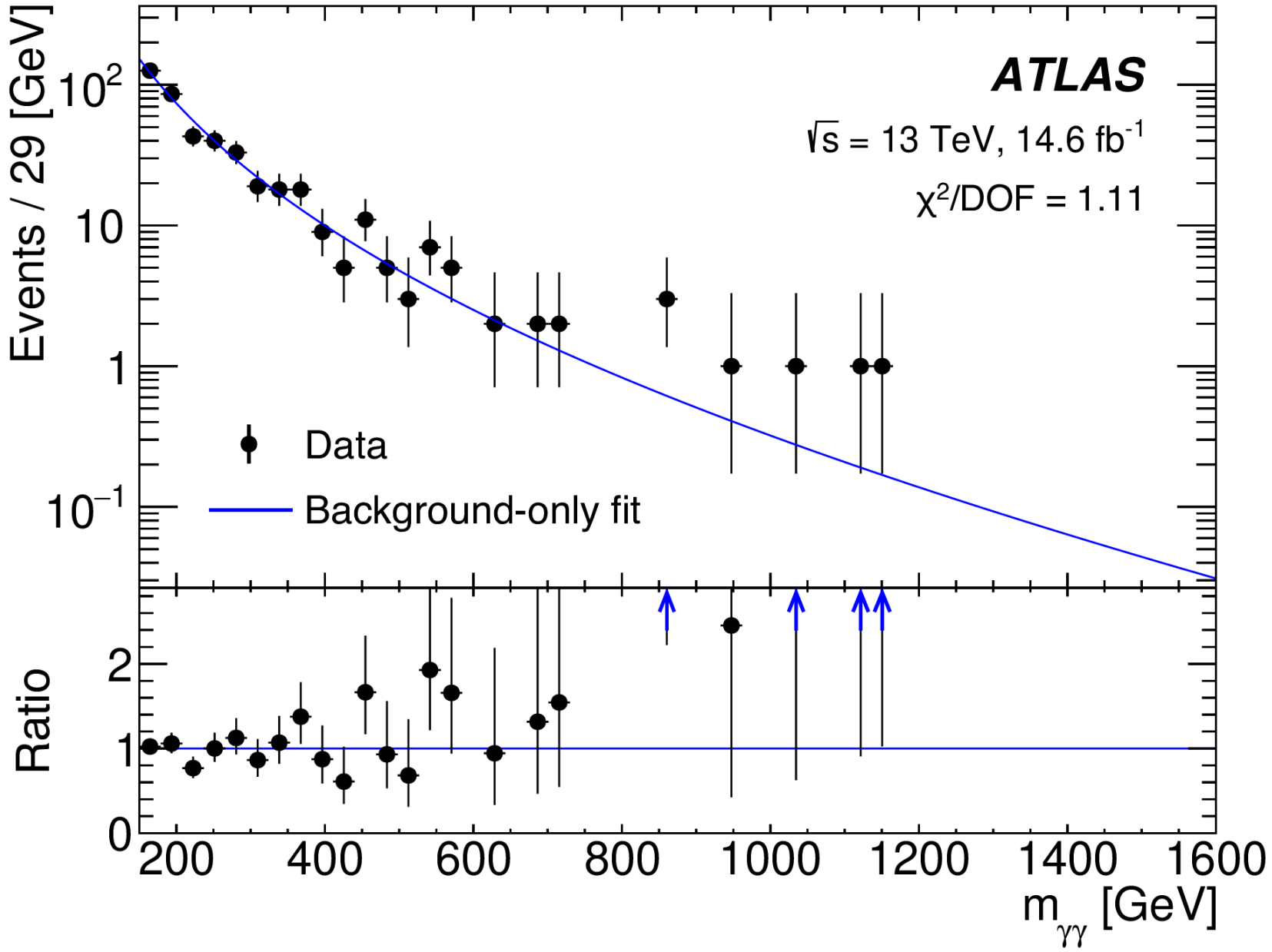

Search results

JHEP 07 (2023) 234

441 events observed

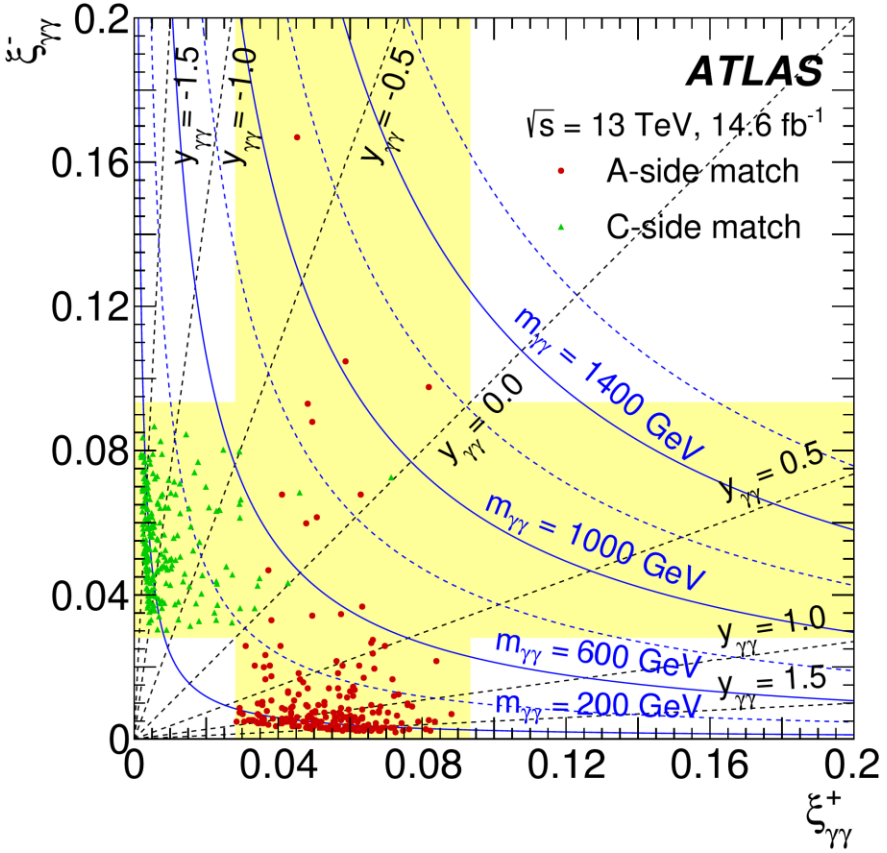

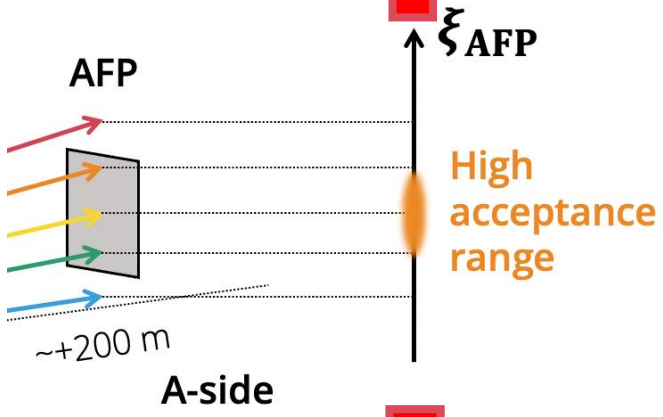

No double matching

Dominant systematic uncertainty: AFP global alignment

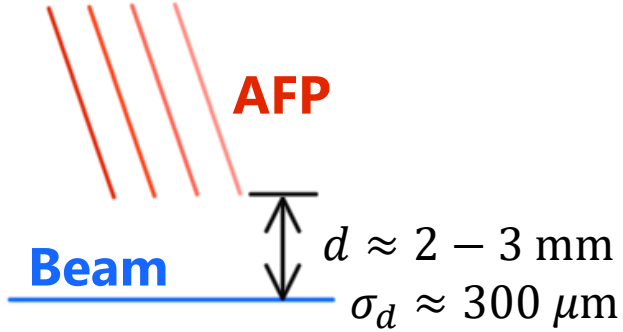

Systematics

Source	Uncertainty
Signal yield uncertainty	
Pile-up reweighting	$^{+2.7}_{-2.6}$%
Luminosity	±2.4%
Photon identification efficiency	$^{+1.6}_{-1.5}$%
Photon isolation efficiency	±1.9%
Beam optics between ATLAS central and AFP detectors	$^{+0.8}_{-3.4}$%
AFP global alignment	$^{+10.0}_{-8.6}$%
Proton reconstruction efficiency	$^{+3.0}_{-2.2}$%
Showering in the AFP	$^{+0.0}_{-6.6}$%
Background modelling (mass-dependent)	±(0.02–0.7) events
Signal modelling	
Photon energy resolution	$^{+14.1}_{-4.8}$%
Photon energy scale	±(0.5–1.0)%
Signal cross-section uncertainty	
Soft survival factor (exclusive process)	±2%
Soft survival factor (single-dissociative process)	±10%
Soft survival factor (double-dissociative process)	±50%

JHEP 07 (2023) 234

Exclusion limits

JHEP 07 (2023) 234

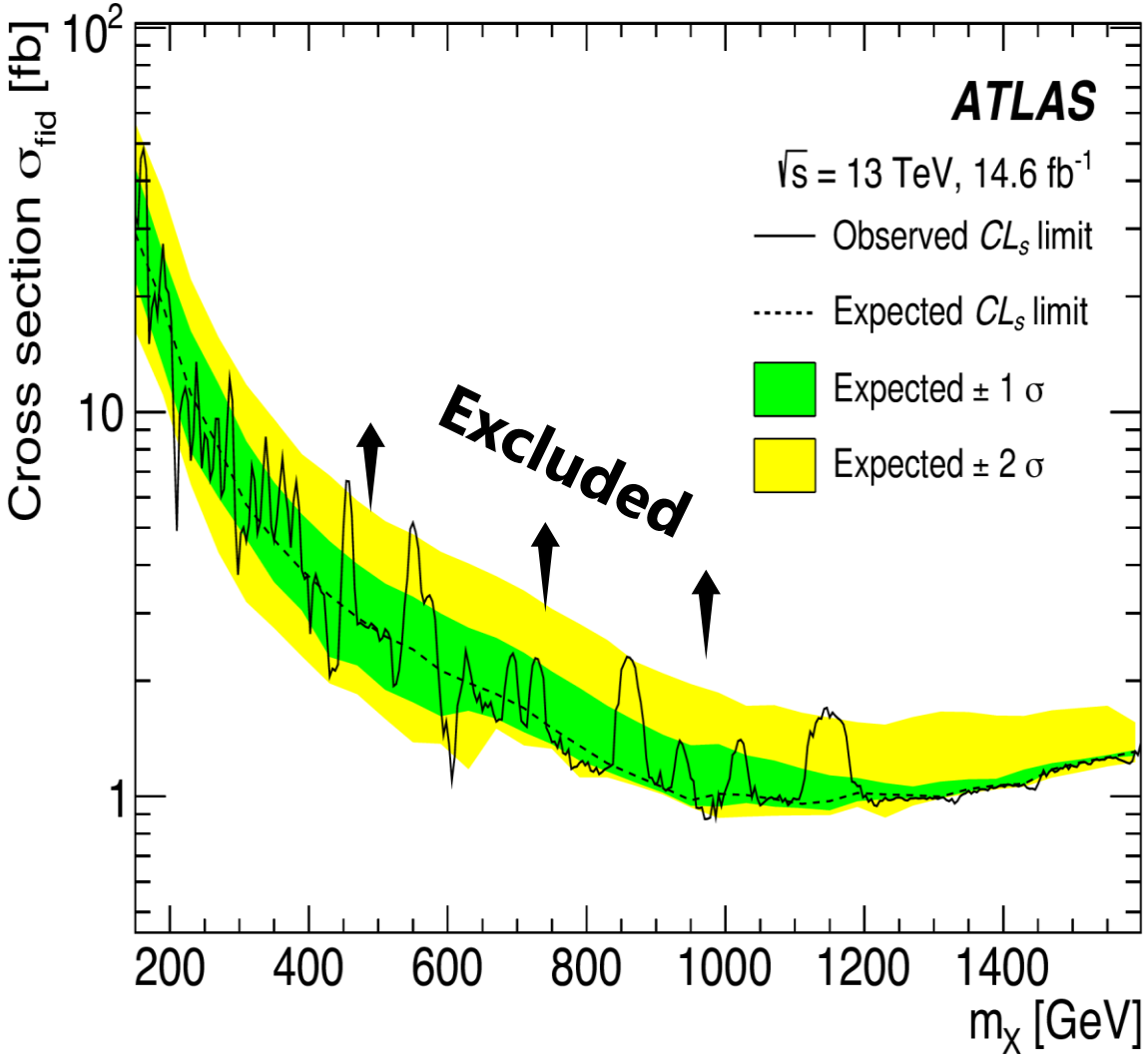

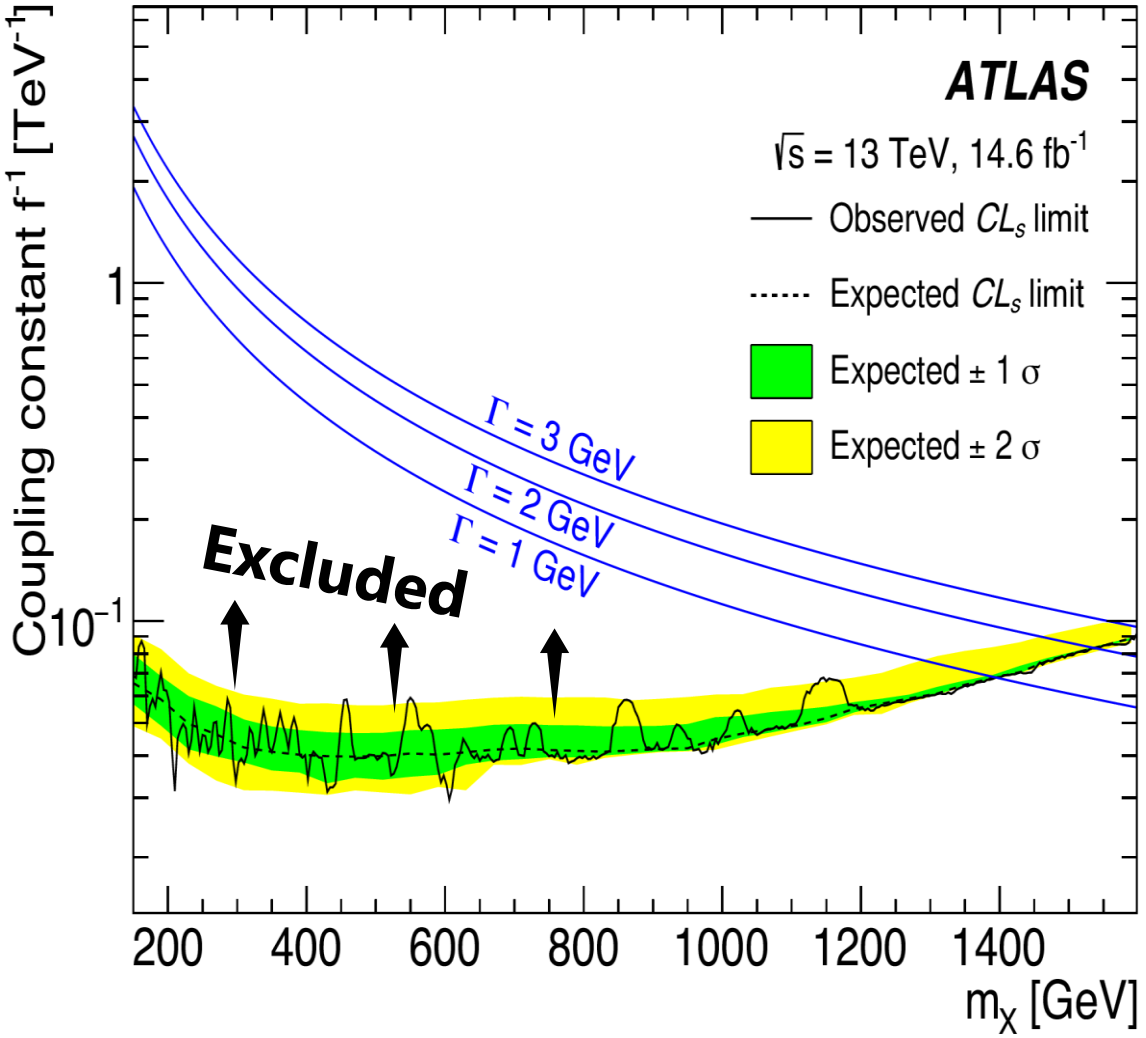

Comparison with previous $\gamma\gamma \rightarrow \gamma\gamma$ results and extrapolation (separating systematic and statistical uncertainties)

ALP-photon coupling ($1/\Lambda_a = 4/f$)

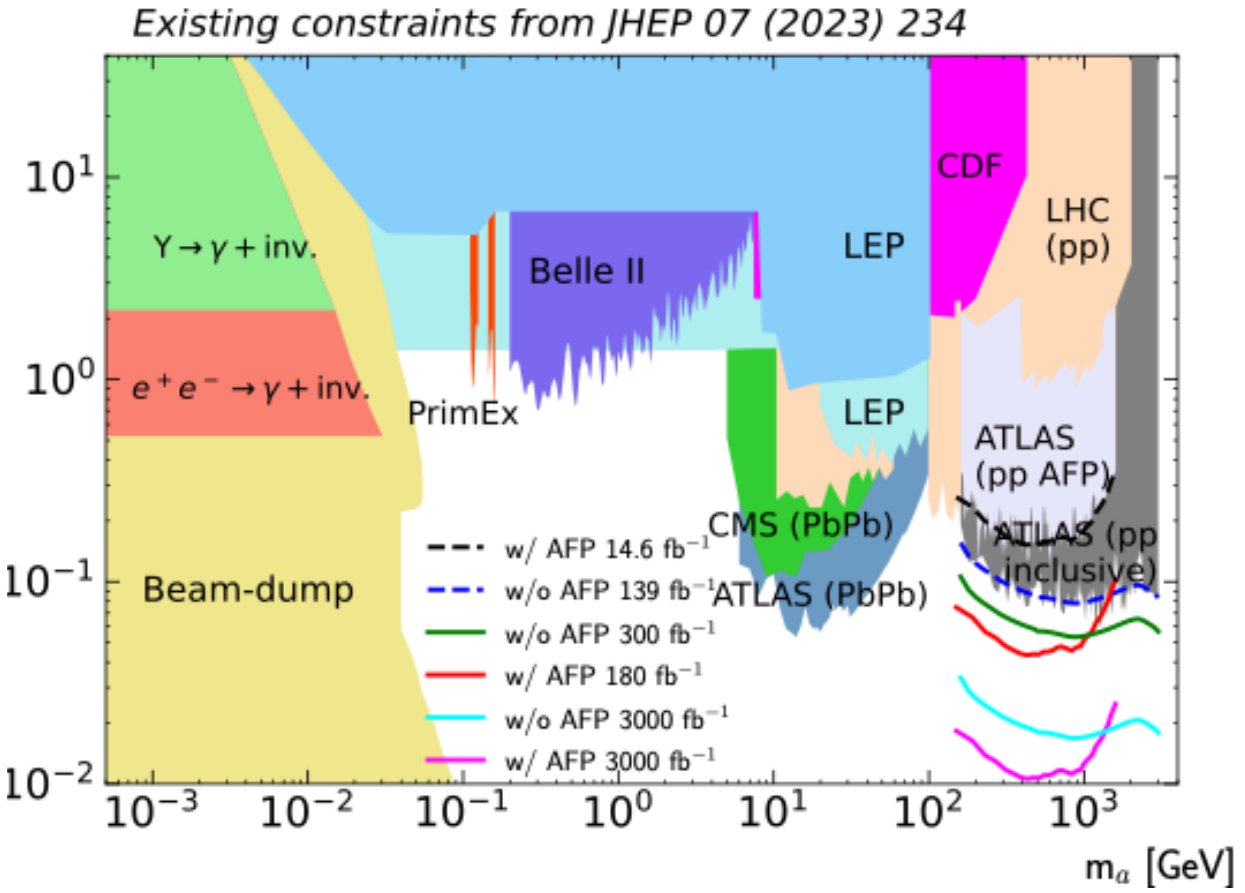

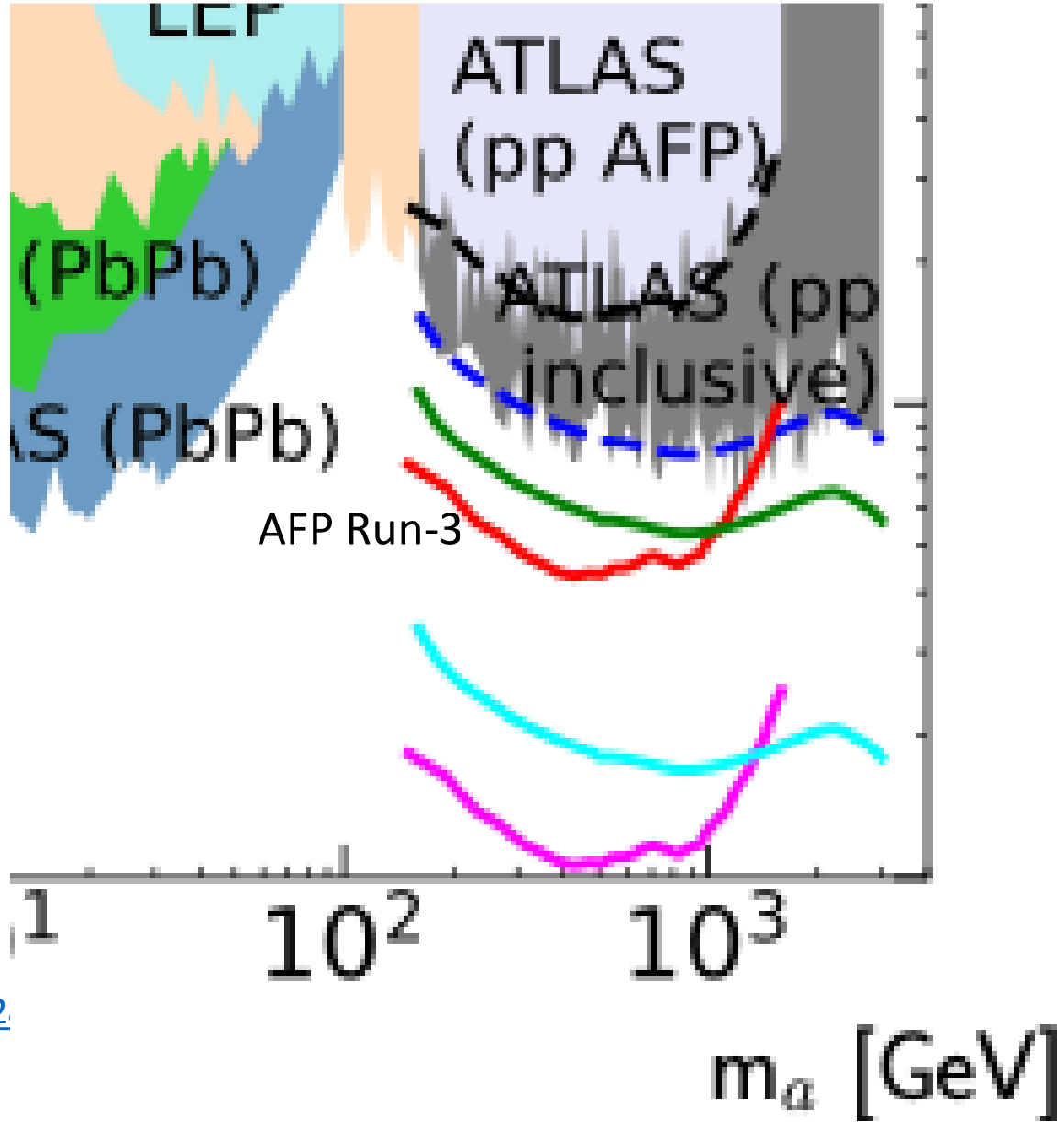

https://atlas.web.cern.ch/Atlas/GROUPS/PHYSICS/PAPERS/EXOT-2019-2
https://cds.cern.ch/record/2890623

Conclusions

- **ATLAS has several photoproduction results based on LHC Run-2 data (taken 2015-2018) from Pb+Pb and pp interactions:**
  - Differential light-by-light, and limit on Axion-Like Particle
  - Measurements of jet production
  - Charged hadron yields in photonuclear collisions
  - Observation of the $\gamma\gamma \rightarrow \tau\tau$ process and anomalous magnetic moment
  - Search for magnetic monopoles
  - Observation of photon-induced WW production

- **ATLAS-AFP has photoproduction results from 2017 data taking, in co-incidence with ATLAS central detector data:**
  - Di-lepton measurement with proton tag
  - Di-photon search with proton tag, and limit on Axion-Like-Particle

- **Outlook LHC Run-3 (2022-2025): already now as much data recorded as in whole Run-2. Many further photoproduction results – stay tuned.**

Supplement

AFP detectors at -200m and +200m from IP

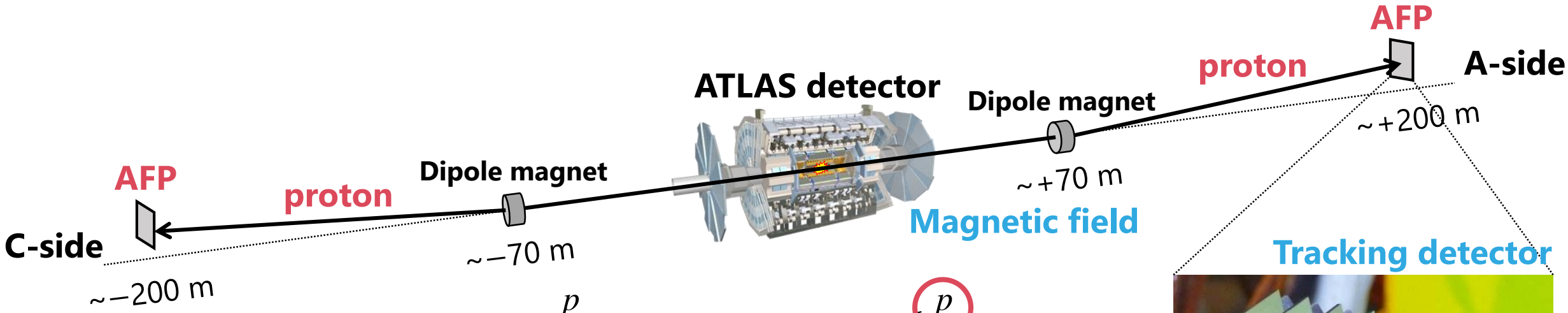

Example:
Register protons from light-by-light scattering

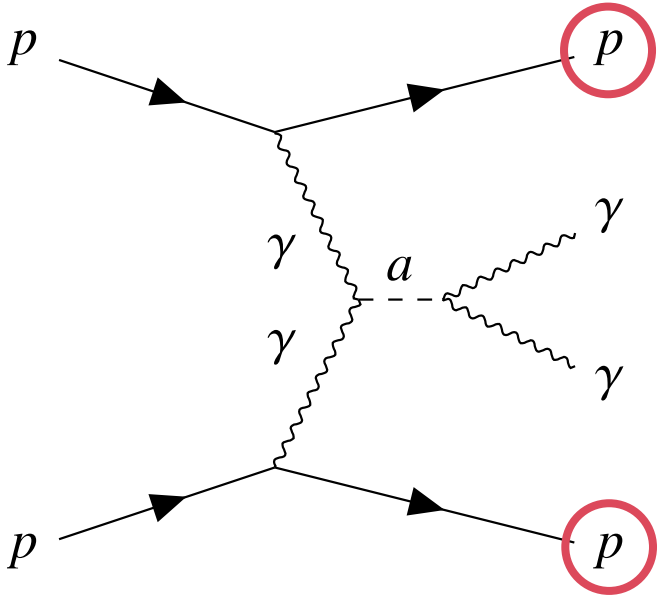

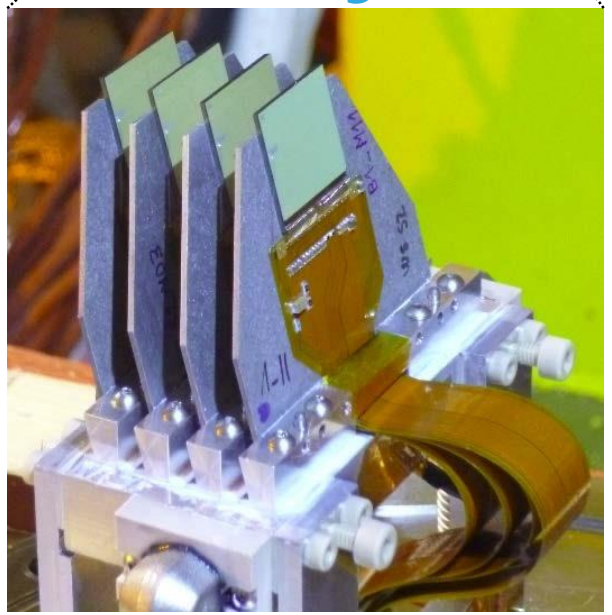

AFP detector

In $\gamma\gamma \to \gamma\gamma$ events, final state proton can be intact, record ATLAS forward proton (AFP) detectors

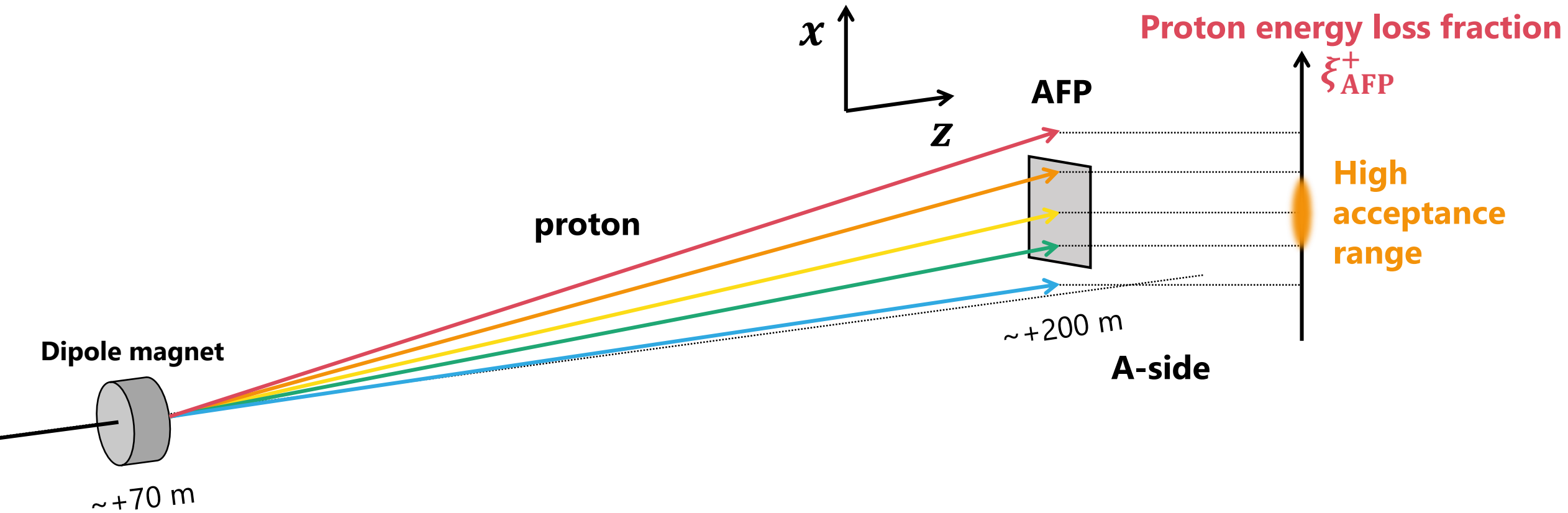

AFP detector

- **Each side of the AFP systems is referred to as an arm.**
- **For tracking the Silicon Tracker (SiT) is used, which consists of four layers of silicon pixel detectors.**
- **Only FAR stations equipped with the Time-of-Flight (ToF) detectors.**

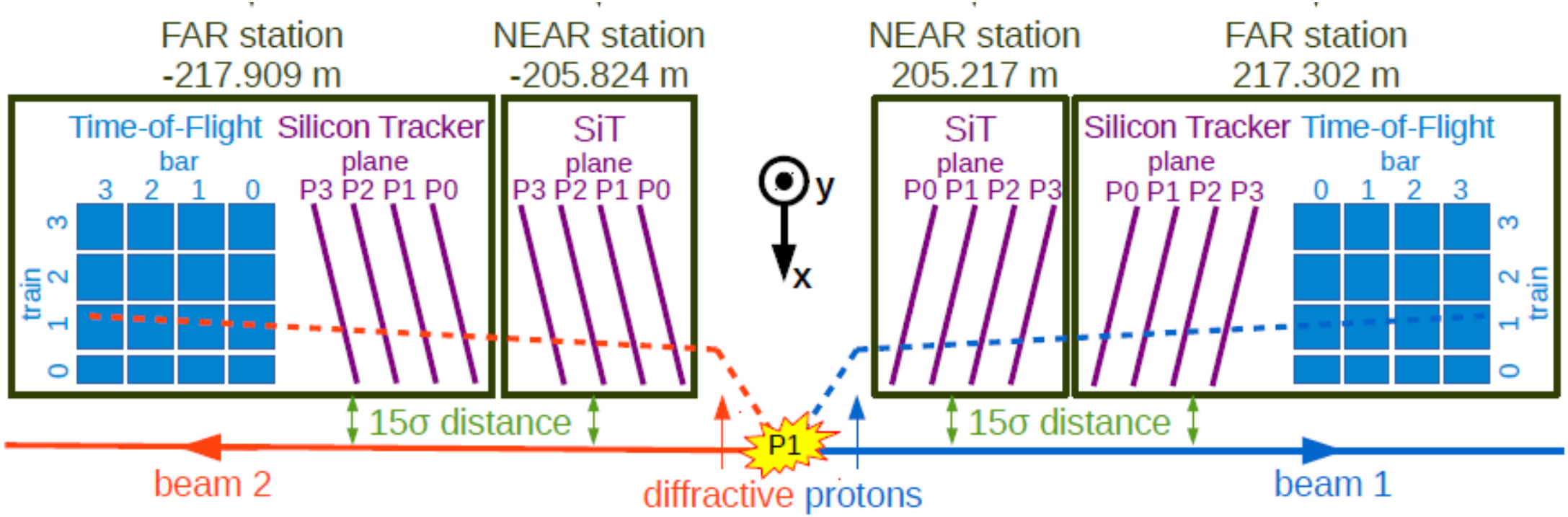

AFP Run-2 data-taking in 2017: 32 fb^{-1} at 13 TeV

https://twiki.cern.ch/twiki/bin/view/AtlasPublic/LuminosityPublicResultsRun3

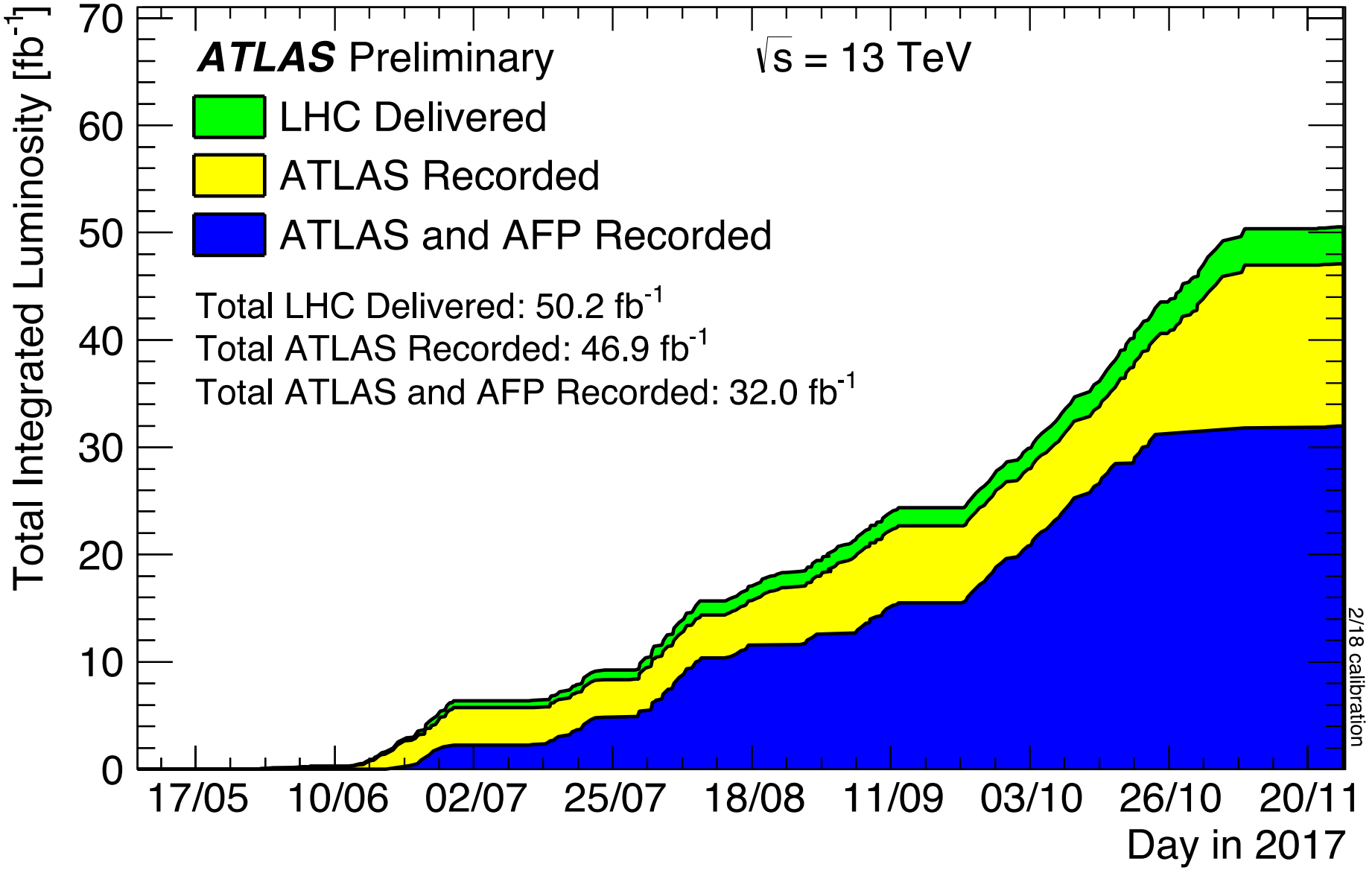

Used for this analysis 14.6 fb^{-1}

Purpose and main strategy

Diphoton resonance search using AFP

Select events where ξ_{AFP} is close to $\xi_{\gamma\gamma}$: matching

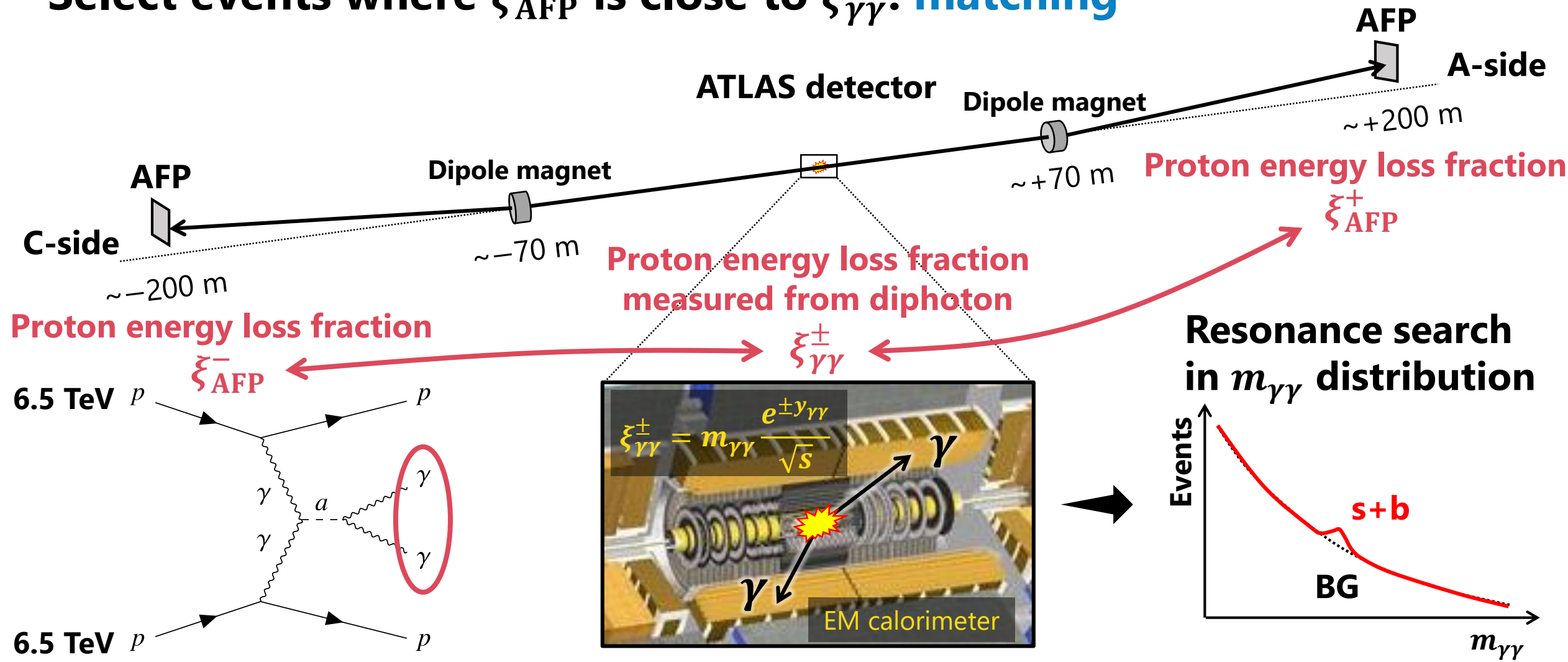

Event selection

1. **Require diphoton to be back-to-back**

   Acoplanarity $A_{\phi}^{\gamma\gamma} \equiv 1 - \frac{|\Delta\phi|}{\pi} < 0.01$

2. **Require ξ_{AFP} in the high acceptance range**

   $0.035 < \xi_{\mathrm{AFP}} < 0.08 \rightarrow \xi_{\gamma\gamma}$ range is also limited

3. **<u>At least one</u> matching proton**

   $|\Delta\xi| \equiv \left|\xi_{\mathrm{AFP}} - \xi_{\gamma\gamma}\right| < 0.004 + 0.1\xi_{\gamma\gamma}$

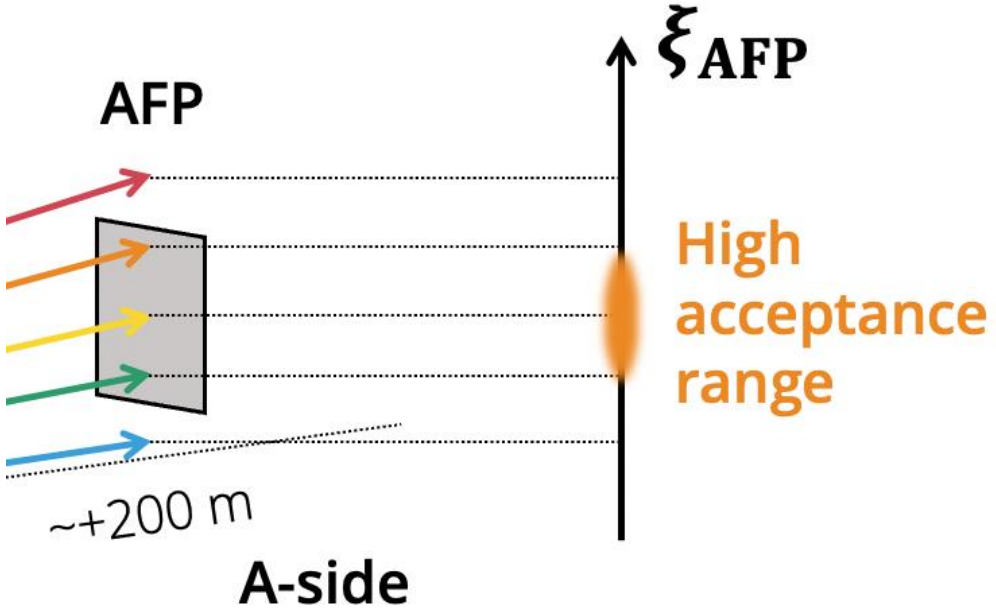

Selection efficiency as a function of ALP mass

Exclusive event

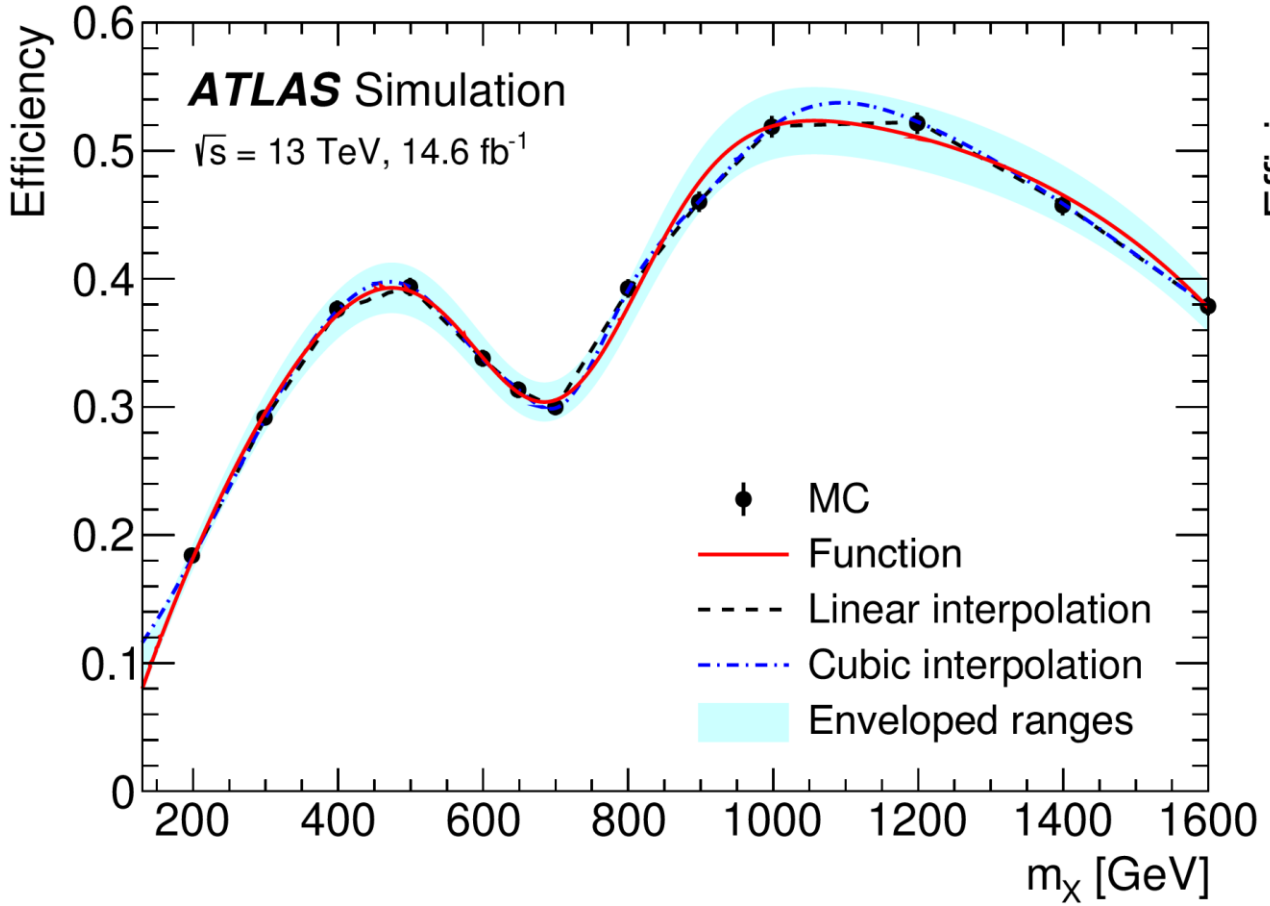

Single-dissociative (SD) event

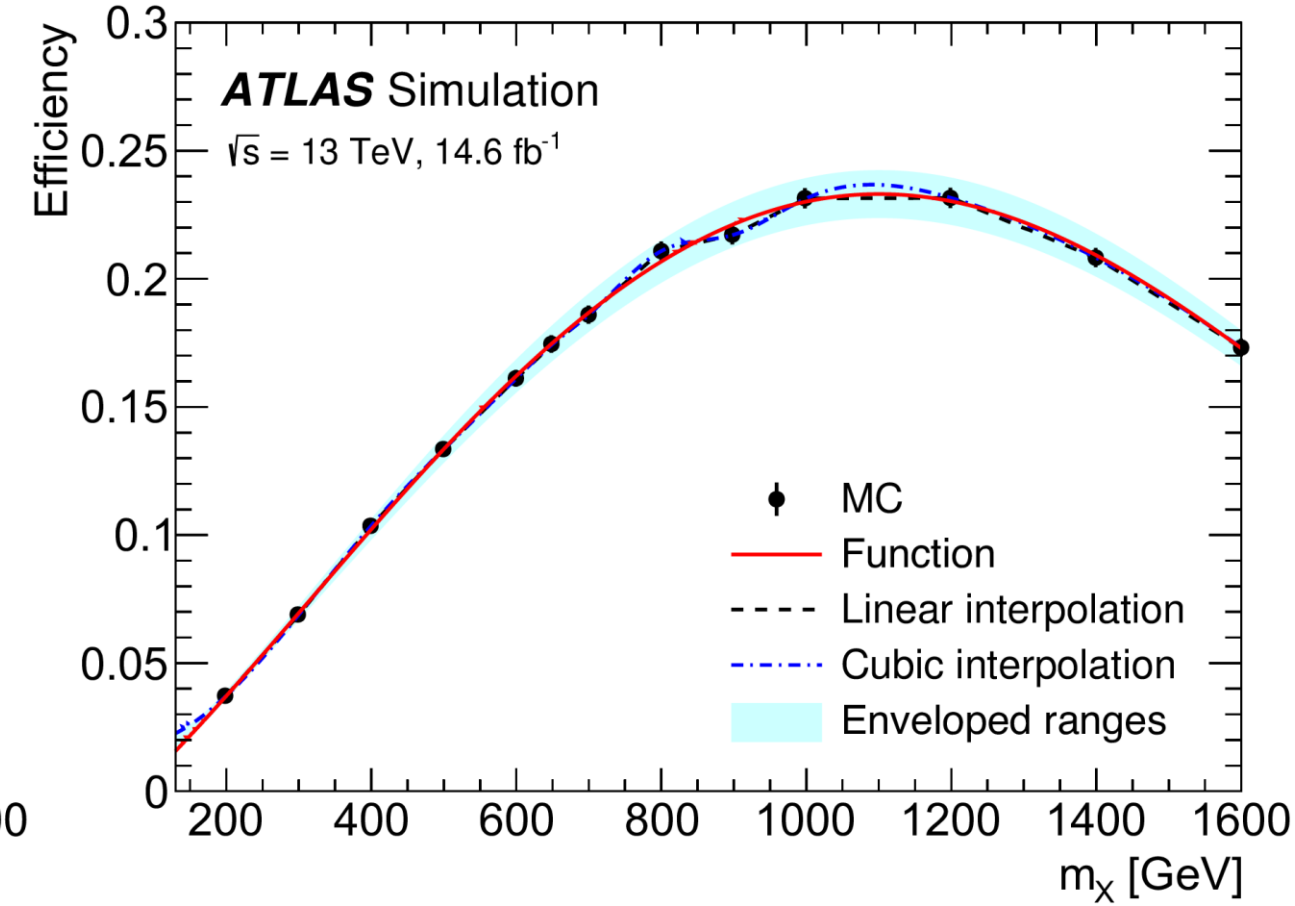

Background sample generation

Photons and protons are recorded for each event

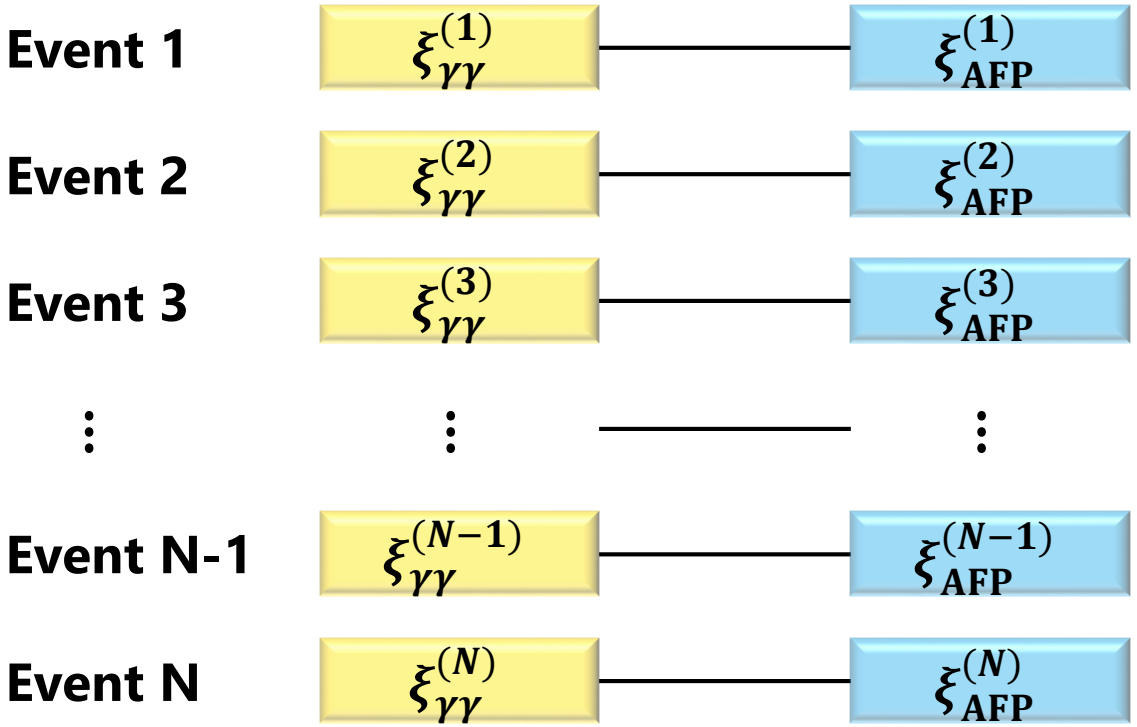

Background sample generation

Photons and protons are recorded for each event

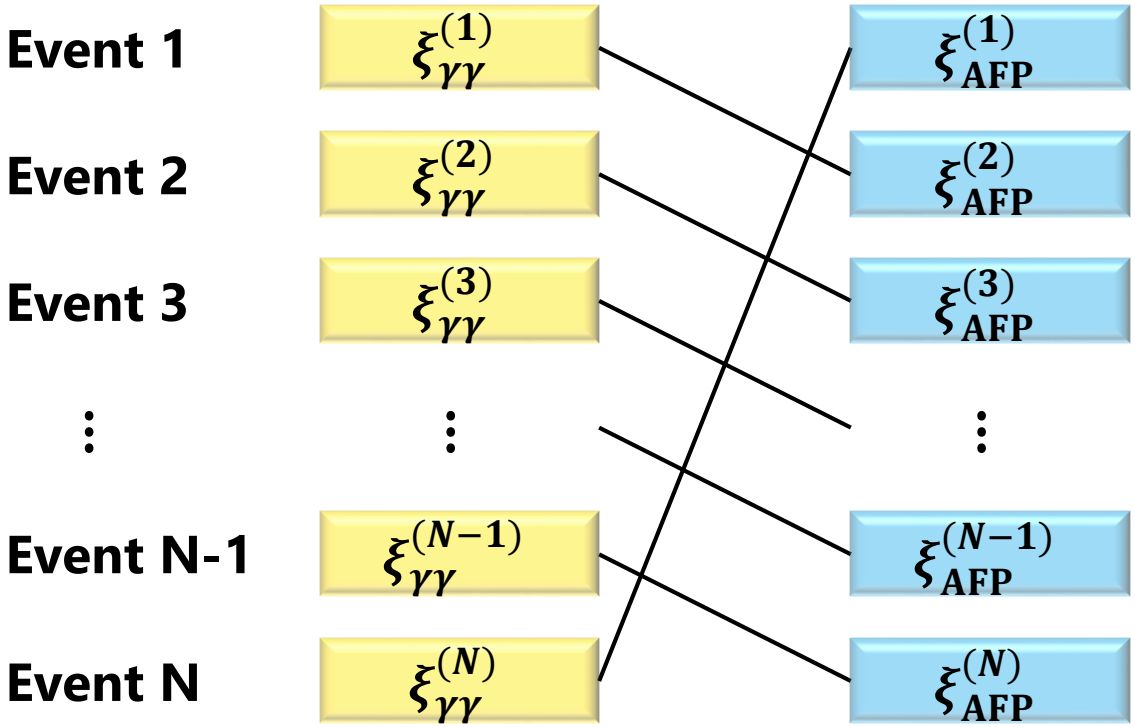

Reassignment of protons to diphotons

→ **Pure combinatorial BG sample**

Background sample generation

All other combination of the reassignment

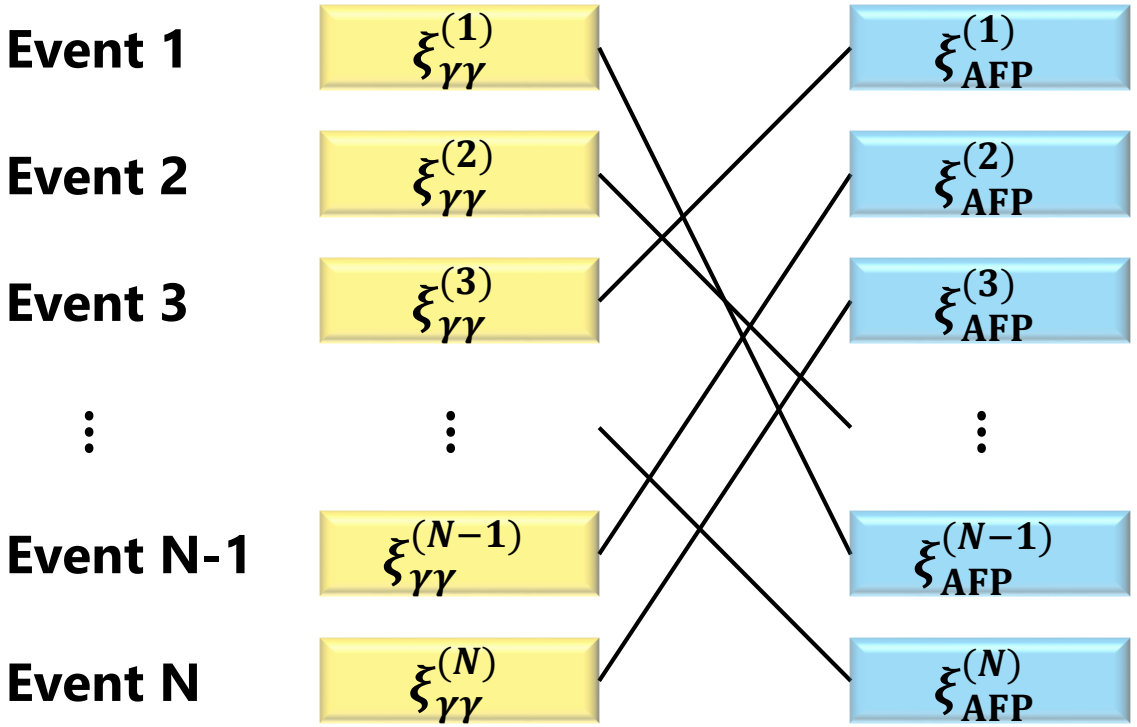

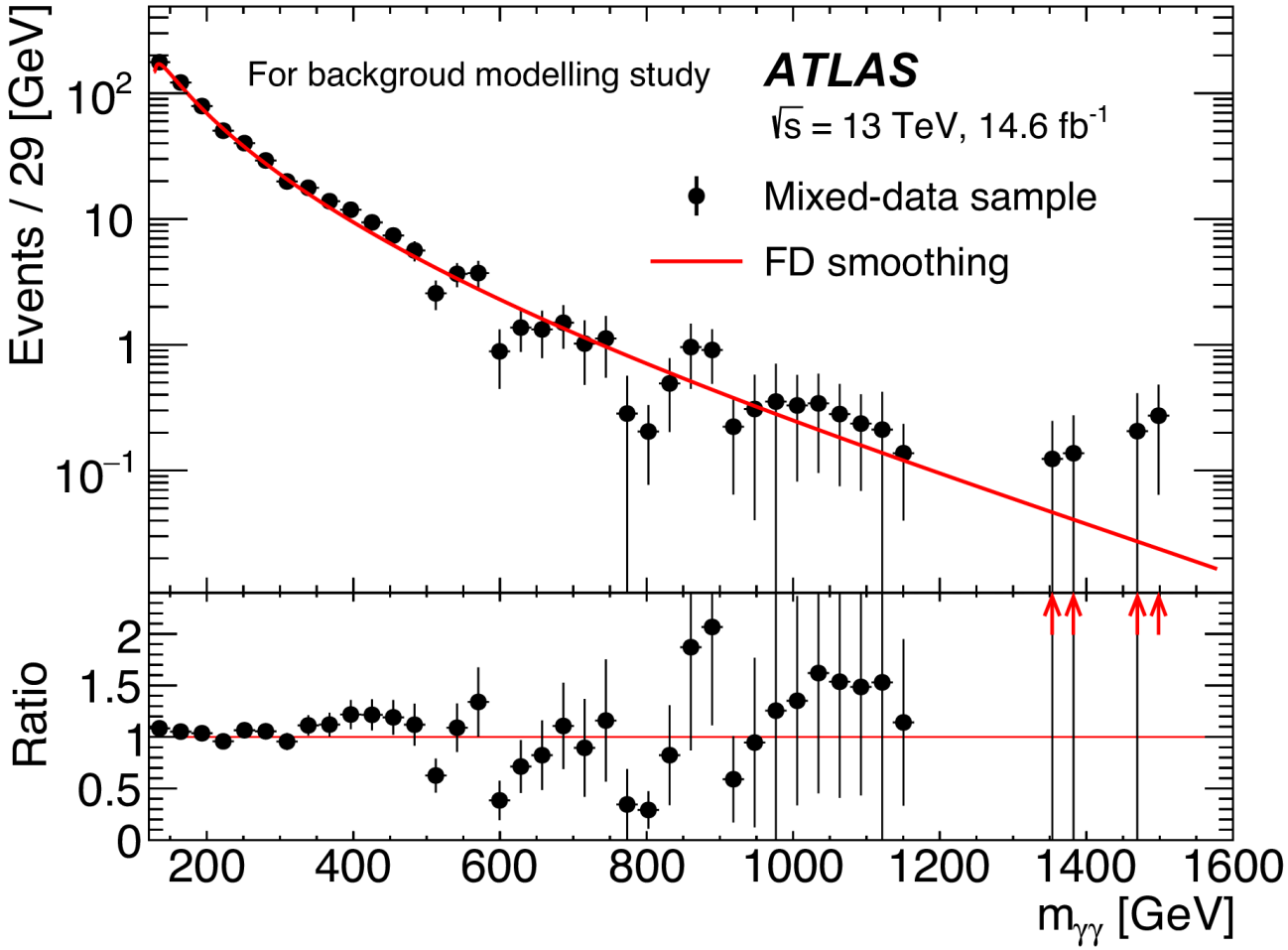

Functional Decomposition (FD)